4-7-2022

Combined effects of aerobic exercise and 40-Hz light flicker exposure on early cognitive impairments in Alzheimer's disease of 3×Tg mice

Sang-Seo Park

Hye-Sang Park

Change-Ju Kim

Seung-Soo Baek

Song-young Park

See next page for additional authors

Authors

Sang-Seo Park, Hye-Sang Park, Change-Ju Kim, Seung-Soo Baek, Song-young Park, Cody Anderson, Myung-Ki Kim, Ik-Ryeul Park, and Tae-Woon Kim

Combined effects of aerobic exercise and 40-Hz light flicker exposure on early cognitive impairments in Alzheimer's disease of 3xTg mice

Sang-Seo Park,[1]† Hye-Sang Park,[2]† Chang-Ju Kim,[2] Seung-Soo Baek,[3] Song-Young Park,[1] Cody Anderson,[1] Myung-Ki Kim,[4] Ik-Ryeul Park,[5] and Tae-Woon Kim[5]

[1]*School of Health and Kinesiology, University of Nebraska at Omaha, Omaha, Nebraska;*

[2]*Department of Physiology, College of Medicine, KyungHee University, Seoul, Republic of Korea;*

[3]*Department of Exercise & Health Science, Sangmyung University, Seoul, Republic of Korea;*

[4]*Division of Global Sport Studies, Korea University, Sejong, Republic of Korea; and*

[5]*Department of Human Health Care, Gyeongsang National University, Jinju, Republic of Korea*

†S-S. Park and H-S. Park contributed equally to this work.

Abstract

Alzheimer's disease (AD) is a progressive degenerative brain disease and the primary cause of dementia. At an early stage, AD is generally characterized by short-term memory impairment, owing to dysfunctions of the cortex and hippocampus. We previously reported that a combination of exercise and 40-Hz light flickering can protect against AD-related neuroinflammation, gamma oscillations, reduction in Ab, and cognitive decline. Therefore, we sought to extend our previous findings to the 5-mo-old 3xTg-AD mouse model to examine whether the same favorable effects occur in earlier stages of cognitive dysfunction. We investigated the effects of 12 wk of exercise combined with 40-Hz light flickering on cognitive function by analyzing neuroinflammation, mitochondrial function, and neuroplasticity in the hippocampus in a 3xTg-AD mouse model. Five-month-old 3xTg-AD mice performed 12 wk of exercise with 40-Hz light flickering administered independently and in combination. Spatial learning and memory, long-term memory, hippocampal Ab, tau, neuroinflammation, proinflammatory cytokine expression, mitochondrial function, and neuroplasticity were analyzed. Ab and tau proteins levels were significantly reduced in the early stage of AD, resulting in protection against cognitive decline by reducing neuroinflammation and proinflammatory cytokines. Furthermore, mitochondrial function improved, apoptosis was reduced, and synapse-related protein expression increased. Overall, exercise with

40-Hz light flickering was significantly more effective than exercise or 40-Hz light flickering alone, and the improvement was comparable to the levels in the nontransgenic aged-match control group. Our results indicate a synergistic effect of exercise and 40-Hz light flickering on pathological improvements in the hippocampus during early AD-associated cognitive impairment.

NEW & NOTEWORTHY Exercising in a 40-Hz light flicker environment was more effective than exercise or 40-Hz light flicker alone. This synergistic effect may prevent cognitive dysfunction by inhibiting Ab, tau pathway, and neuroinflammation and enhancing neuroplasticity and mitochondrial functions in the hippocampus during early Alzheimer's disease.

Alzheimer's disease; cognitive function; exercise; hippocampus; 40-Hz light flicker

INTRODUCTION

Alzheimer's disease (AD) is a progressive degenerative brain disease and the primary cause of dementia. In early AD, memory impairment, which affects the ability to recall recent experiences, results from cortex and hippocampal dysfunction. The lesion gradually spreads, primarily to the association cortex, thereby impairing overall cognitive function. It is known that the pathology of AD includes amyloid-b (Ab) accumulation from amyloid plaques, tau aggregation by nerve fiber entanglement, and brain atrophy from the loss of neurons and synapses (1). These processes support the amyloid cascade hypothesis, which proposes that changes in Ab initiate AD, and a series of events, including the accumulation of a toxic form of tau, which ultimately triggers downstream neuronal death (2, 3). Ab deposition and tau protein expression ultimately results in a loss of synaptic function, mitochondrial damage, and microglia and astrocyte activation (4). This hypothesis has been supported by previous studies, which have suggested that Ab production and aggregation start to increase several years before the onset of symptoms. In addition, along with the accumulation of

Ab, synapse degradation has been shown to cause cognitive decline and disease progression in early AD (1, 5). Previous studies also suggest that the activation of microglia and astrocytes around amyloid plaques significantly contributes to AD-related inflammation (6, 7). Neuroinflammation is generally mediated by the release of reactive oxygen species (ROS), nitric oxide, proinflammatory chemokines, cytokines, and potentially includes the release of neurotoxin molecules from activated glia (8). The overexpression of these mediators induces nerve damage in AD and other neurodegenerative disorders by various mechanisms (9). Furthermore, neuroinflammation mediated by oxidative stress damage, which is associated with mitochondrial dysfunction, has been suggested to be one of the major factors contributing to the early stages of AD (10). Mitochondria are known to be essential for maintaining aspects of cellular homeostasis in neurons, such as during synapse activation. In addition, mitochondrial dysfunction, such as morphological abnormalities, reduced respiratory function, and excessive ROS production, has been observed in the pathophysiological process of neurodegenerative dis- eases, such as AD (11–16).

Although various AD treatments are currently under development, there are no effective pharmacological treatments that have been created at this time. Previous studies have suggested that exercise positively alters brain function in various age groups and effectively reduces the risks of AD, such as neuroinflammation and cell death, which may slow down cognitive impairment in AD and later life (17, 18). Despite these findings, the beneficial effects of exercise are limited to either a delay or a reduction in cognitive decline, rather than a complete improvement in cognitive function in AD. Therefore, it has been suggested that additional treatments are needed to complement the effects of exercise. Previous studies have reported that 40- Hz light flicker treatment improves AD-related pathological factors and cognitive function (19–21). Ferreira and Castellano (22) suggested that 40–120 Hz gamma oscillations appear to improve attention and cognitive function in neurodegeneration. Recently, we performed a study using a combination of exercise and 40-Hz light

flicker exposure on end stage (12 mo) 3xTg-AD mice, which tend to have severe cognitive dysfunction, and we found that this novel treatment showed positive results in the hippocampus (23), but it is unknown if these results transfer to early stage (5 mo) 3xTg-AD mice, which tend to be in less advanced stages of cognitive dysfunction. Therefore, the purpose of this study was to investigate the effects of 12 wk of exercise, combined with 40-Hz light flickering, on cognitive function in an early stage (5 mo) 3xTg-AD mouse model. We hypothesized that the combination of aerobic exercise with 40-Hz light flickering may be a favorable treatment for improving cognitive function and related pathological factors in the early stages of AD.

MATERIALS AND METHODS

Animals

All animal experiments were performed in accordance with the guidelines of the National Institutes of Health and the Korean Academy of Medical Science. The study proto- col was approved by the KyungHee University Institutional Animal Care and Use Committee (approval number KHUASP [SE]-17–103).

Five-mo-old male 3xTg mice were kept under the following conditions: arbitrary adjustment of food and water, 25 ± 1°C, and light from 7 AM to 7 PM. Mice were randomly divided into a wild-type (CON) group, 3xTG-AD (AD) group, 3xTg-AD and 40-Hz light flicker (AD þ 40) group, 3xTg-AD and exercise (AD þ EX) group, and 3xTg-AD and exercise with 40-Hz light flicker (AD þ 40 þ EX) group (n = 10/ group). We only included homozygous male 3xTg mice in this study because of the limited availability of female 3xTg mice and because male 3xTg mice perform poorer than females in spatial memory (25). All test animals were 5 mo of age. The genotype of each animal was confirmed by a PCR analysis of DNA from tail biopsies. BrdU (Sigma, St. Louis, MO) was administered intraperitoneally (ip) at 100 mg/kg/ day for 7 days for 4 wk before killing the animal to observe neurogenesis.

Exercise Protocol and Exposure to 40-Hz Light Flickering

Exercise sessions were initiated in 5-mo-old 3xTg mice. Animals in the exercise groups exercised on a treadmill made for animal use once daily in the dark, 6 days per wk for 12 consecutive weeks. For acclimation, mice were subjected to 5 min of warm up at a 0º incline at 3 m/min, 30 min of the main exercise at 10 m/min, and 5 min of cool down at 3 m/min for the first 3 wk. Subsequently, mice were subjected to 40 min of the main exercise at 11 m/min from *wk 4* to *6*, 50 min of the main exercise at 12 m/min from *wk 7* to *9*, and 50 min of the main exercise at 13 m/ min from *wk 10* to *12*. During treadmill running, electrical stimulation was removed to minimize stress. The exposure time to 40-Hz light flickering was the same as the exercise time (Fig. 1).

Preparation of Tissue Samples

Mice were euthanized immediately after the behavior test. To prepare brain slices, the animals were fully anesthetized with ethyl ether, perfused transcardially with 50 mM phosphate-buffered saline (PBS), and then fixed with a freshly prepared solution of 4% paraformaldehyde in 100 mM phosphate buffer (pH 7.4). The brains were then removed, post- fixed in the same fixative overnight, and transferred to a 30% sucrose solution for cryoprotection. Coronal sections with 40-μm thickness were created using a freezing micro- tome (Leica, Nussloch, Germany). From each group of 10 animals, five were used for immunohistochemistry and five for Western blotting and analyses of mitochondrial function. The hippocampal for Western blot analyses was immediately stored at –80ºC until use.

Behavioral Analysis

Morris water maze.

The Morris water maze test was conducted to measure spatial learning and memory ability. The test animals were acclimated by swimming freely for 60 s in a pool without a platform 1 day before the start of training. The educational training was performed three times a day for 5 days with a platform. If the animal was

unable to find the location of the platform within 60 s, the experimenter guided the ani- mal to the platform. Then, the animal remained on the platform for 30 s. A probe trial was conducted 24 h after the training session; free swimming for 60 s without a platform was automatically evaluated by video tracking to determine whether the memory of the previous platform was retained or not.

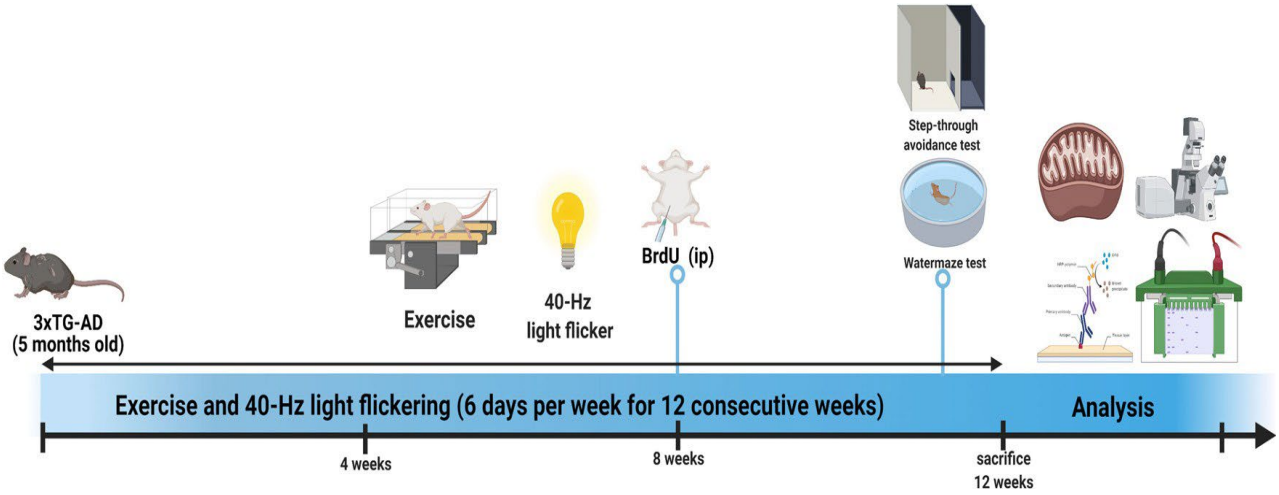

Figure 1. Study design and timeline. Exercise groups exercised on a treadmill made for animal use once daily in the dark, 50 min/days, 6 days/wk for 12 consecutive weeks the exposure time to 40-Hz light flickering was the same as the exercise time.

Step-through avoidance test.

A step-through avoidance test was conducted to measure long-term memory. On the first day of training, the test ani- mal was placed on a platform illuminated by a halogen light bulb, and the box door was opened. When the test animal entered the dark box, the door was closed, and the animal was allowed to stay for 20 s. This process was performed twice. In the third or final trial, the door was closed, and a foot shock at 0.2 mA current and 2 s in duration was administered once. After 24 h, the test animal was placed on a plat- form illuminated with a halogen light bulb. When the box door was opened, the latency to enter the dark box was measured. All times exceeding 300 s were recorded as 300 s.

Immunohistochemistry

To visualize Aβ, neuroinflammation, and cell differentiation,

immunohistochemistry was performed to detect glial fibrillary acidic protein (GFAP) and ionized calcium-binding adaptor protein-1 (Iba-1) with antigen retrieval in CA1 and the dentate gyrus (DG), doublecortin (DCX) in the DG, and Ab in the CA1 region of the hippocampus. The sections were incubated in PBS for 10 min and then washed three times for 3 min in PBS. The sections were then incubated in 1% H_2O_2 for 15 to 30 min. Sections were obtained from each brain and incubated overnight with goat anti-DCX antibody (1:500; Santa Cruz Biotechnology, Dallas, TX), mouse purified anti- b-amyloid antibody (1:200; Biolegend, San Diego, CA), goat anti-GFAP (1:500; Abcam, Cambridge, UK), and rabbit Iba-1 (1:500; Abcam), followed by incubation with biotinylated goat, mouse, rabbit secondary antibody (1:200; Vector Laboratories, Burlingame, VT) for another 90 min. The secondary antibody was amplified using the Vector Elite ABC kit (1:100; Vector Laboratories). Antibody-biotin-avidin-peroxidase complexes were visualized using the 3,3, Diaminobenzidine (DAB) Substrate kit (Vector Laboratories). The slides were air-dried overnight at room temperature, and the coverslips were mounted using Permount.

Immunofluorescence

NeuN/BrdU-positive cells in the DG were evaluated by immunofluorescence. In brief, the brain sections were permeabilized by incubation in 0.5% Triton X-100 in PBS for 20 min, incubated in 50% formamide-2x standard saline citrate at 65°C for 2 h, denatured in 2 N HCl at 37°C for 30 min, and then rinsed twice in 100 mM sodium borate (pH 8.5). The sections were incubated overnight with rat anti-BrdU anti-body (1:200; Abcam) and mouse anti-NeuN antibody (1:200; Millipore, Temecula, CA). The brain sections were then washed in PBS and incubated with appropriate secondary antibodies for 1 h. The secondary antibodies were anti-mouse IgG Alexa Fluor-488 and anti-rat IgG Alexa Fluor-560.

Quantification of Histology

Quantification of immunohistochemistry and immunofluorescence for the

hippocampus, spanning −3.00 to −3.72 mm from the bregma, was obtained from each brain. Images were captured using a BX51TF microscope (Olympus, Tokyo, Japan) for immunohistochemistry and an FV3000 confocal microscope (Olympus, Tokyo, Japan) for a subsequent Z-section (1 mm) analysis for immunofluorescence. For positive cell counts, images were photographed and quantified hippocampal CA1 and dentate gyrus fields that were randomly chosen from each brain section. A total of two fields were manually analyzed per mouse by one blind experimenter. From each group of 10 animals, 5 were used for immunohistochemistry and immunofluorescence and 2 sections from each group were analyzed, resulting in a total of 10 slices. Quantification of immunohistochemistry and immunofluorescence was calculated by dividing the number of positive cells by the area of CA1 and dentate gyrus.

TUNEL Staining

To visualize DNA fragmentation, TUNEL staining was per- formed using an In Situ Cell Death Detection kit (Roche Diagnostics, Risch-Rotkreuz, Switzerland) according to the manufacturer's protocol. Sections were postfixed in ethanol-acetic acid (2:1), rinsed, incubated with proteinase K (100 mg/mL), and then rinsed again. Next, they were incubated in 3% H_2O_2, permeabilized with 0.5% Triton X-100, rinsed, and incubated in the TUNEL reaction mixture. The sections were rinsed and visualized using Converter-POD with 0.03% DAB, counterstained with Cresyl violet, and mounted onto gelatin-coated slides. The slides were air-dried overnight at room temperature. A coverslip was added using Permount mounting medium.

Western Blotting

Hippocampal tissues were homogenized on ice and lysed in lysis buffer containing 50 mM Tris–HCl (pH 7.5), 150 mM NaCl, 0.5% deoxycholic acid, 1% Nonidet P40, 0.1% sodium dodecyl sulfate, 1 mM PMSF, and leupeptin 100 mg/mL. The protein content was measured using a Colorimetric Protein Assay kit (Bio-Rad, Hercules, CA). Thirty micrograms of protein were separated on sodium dodecyl sulfate-polyacryl-amide gels and transferred onto a nitrocellulose

membrane, which was incubated with mouse β-actin (1:1,000; Santa Cruz Biotechnology), GAPDH (1:3,000; Santa Cruz Biotechnology), t-Akt and p-Akt (1:1,000; Cell Signaling, Danvers, MA), t- GSK3β and p-GSK3β (ser 9) (1:1,000; Cell Signaling), t-Tau and p-Tau (ser202/Thr205, 1:1,000; Thermo Fisher Scientific, Waltham, MA), amyloid precursor protein (APP; 1:1,000; Abcam), adenine nucleotide translocator (ANT1/2, 1:1,000, Proteintech, Rosemont, IL), voltage-dependent anion-selective channel protein (VDAC1, 1:1,000: Bioss, Woburn, MA), cyclophilin D (Cyp-D, 1:1,000; Thermo Fisher Scientific), tumor necrosis factor-α (TNF-α, 1:1,000; Abcam), interleukin-6 (IL-6, 1:700; Abcam), Bcl-2 and cytochrome C (1:1,000; Santa Cruz Biotechnology), Bax (1:1,000; Cell Signaling), cleaved cas-pase-3 (1:700; Cell Signaling), brain-derived neurotrophic fac- tor (BDNF; 1:1,000; Alomone, Jerusalem, Israel), postsynaptic density protein 95 (PSD95, 1:1,000; Cell Signaling), synaptophysin (1:1,000; Abcam), β-actin and GAPDH (1:3,000; Santa Cruz Biotechnology), and COX IV (1:1,000, Cell Signaling) primary antibodies. Horseradish peroxidase-conjugated secondary anti-mouse antibodies were used for Bcl-2, p-Tau, cytochrome C, β-actin, and GAPDH; anti-rabbit conjugated secondary antibodies were used for t-Akt, p-Akt, t-tau, p-tau, t-GSK3β, APP, ANT1/2, VDAC1, Cyp-D, Bax, cleaved caspase-3, BDNF, PSD95, synaptophysin, and COX IV.

Isolation of Hippocampal Mitochondria

Mitochondria were isolated from the mouse brain using a Mitochondria Isolation kit for Tissue (Thermo No. 89801; Thermo Fisher Scientific) according to the manufacturer's instructions. Briefly, homogeneous suspensions of hippocampal tissue were prepared using a prechilled homogenizer (T 10 Basic Ultra-Turrax; Ika, Staufen im Breisgau, Germany). The hippocampal suspensions were spun at 1,000 *g* for 5 min at 4°C. The pellet was suspended in 800 µL of bovine serum albumin/reagent A solution and incubated for 2 min before adding 10 µL of isolation reagent B. After incubation for 5 min with intermittent vortexing, 800 µL of reagent C was added. The resulting cell lysate was centrifuged at 700 *g* for 10 min at 4°C, after which the supernatant was transferred to a new tube and spun at 3,000 *g* for

15 min at 4°C. The supernatant (cytosolic fraction) was collected for analysis. After washing with mitochondrial isolation reagent C, the mitochondrial pellet was lysed with 2% CHAPS in Tris-buffered saline containing protease inhibitors. The samples were stored at −80°C until use.

Mitochondrial Ca^{2+} Retention Capacity

The mitochondrial calcium retention capacity was tested to assess the susceptibility of the permeability transition pore (PTP) to opening. Briefly, after grinding the hippocampal tis- sue, overlaid traces of changes in fluorescence induced by Calcium Green-5 N were measured continuously (ΔF/min) at 37°C during *state 4* respiration using a Spex FluoroMax 4 spectrofluorometer (Horiba Scientific, Edison, NJ). After establishing the background ΔF (hippocampal tissue in the presence of 1 mM Calcium Green-5 N, 1 U/mL hexokinase, 0.04 mM EGTA, 1.5 nM thapsigargin, 5 mM 2-deoxyglucose, 5 mM glutamate, 5 mM succinate, and 2 mM malate), the reaction was initiated by Ca^{2+} pulses (12.5 nM), with excitation and emission wavelengths set to 506 nm and 532 nm, respectively. The total mitochondrial Ca^{2+} retention capacity before PTP opening (i.e., release of Ca^{2+}) is expressed in units of pmol/mg.

Mitochondrial H_2O_2 Emission

H_2O_2 emission was measured at 37°C (DF/min) during *state 4* respiration (10 μg/mL oligomycin) by continuously monitoring the oxidation of Amplex Red (excitation/emission Λ = 563/ 587 nm) using a Spex FluoroMax 4 spectrofluorometer with 10 μM Amplex Red, 1 U/mL horseradish peroxidase, 10 μg/mL oligomycin, 1 mM malate + 2 mM glutamate (complex I substrates), 3 mM succinate (complex II substrate), and 10 mM glycerol-3-phosphate (lipid substrate). The H_2O_2 emission rate after subtracting the background value from the standard values (standard curve) was calculated from the ΔF/min gradient values and results are expressed in units of pmol/min/mg tissue weight.

Statistical Analyses

Cell counting and optical density quantification were performed using Image-Pro Plus (Media Cyberbetics Inc., Rockville, MD) attached to a light microscope (Olympus). The data were analyzed using one-way analysis of variance, followed by Tukey's post hoc tests. All values are expressed as means ± standard error of the mean, and *P* values <0.05 were considered significant.

RESULTS

Effect of Exercise and 40-Hz Light Flicker on Spatial Working Learning, Memory, and Long-Term Memory in the Early 3xTg-AD

As summarized in Fig. 2, Morris water maze and step- through avoidance tests were performed to evaluate spatial learning, memory, and long-term memory. Spatial learning was evaluated as the time until the animal visited the plat- form. In all groups except the AD group ($P < 0.001$), the time to find the platform was shorter shortened from *day 3*, and there were no differences among treatment groups. With respect to the spatial learning ability, the time to find the platform for each group was as follows: *Day 3*; CON group ($P = 0.022$), AD + 40 ($P = 0.008$), AD + EX ($P = 0.001$), AD + 40 + EX ($P < 0.001$), *Day 4*; CON group ($P = 0.001$), AD + 40 ($P = 0.008$), AD + EX ($P = 0.001$), AD + 40 + EX ($P < 0.001$), *Day 5* ($P < 0.001$). For the spatial memory test at 24 h after 5 days of training, spatial memory was lower in the AD group than in the CON group ($P < 0.001$) and increased in the 40-Hz light flicker group ($P < 0.001$), exercise group ($P < 0.001$), and combination treatment group ($P < 0.001$). The effect of the combination of the two treatments on spatial memory was greater than that of single treatments ($P < 0.001$) and spatial memory in the combined treatment group was equal to or better than that in the nontransgenic CON group ($P = 0.049$). Even long-term memory, as evaluated by the step-through avoidance test, was lower ($P < 0.001$) in the AD group and higher in the 40-Hz light flicker group (P = 0.001), exercise group (P = 0.001), and combination treatment group (P < 0.001) than in the CON group. The combi- nation treatment showed better results than those for the single treatment groups, i.e., the 40-Hz light flicker group (P = 0.004)

and exercise group (P = 0.005), with an increment to the level observed in the nontransgenic CON group.

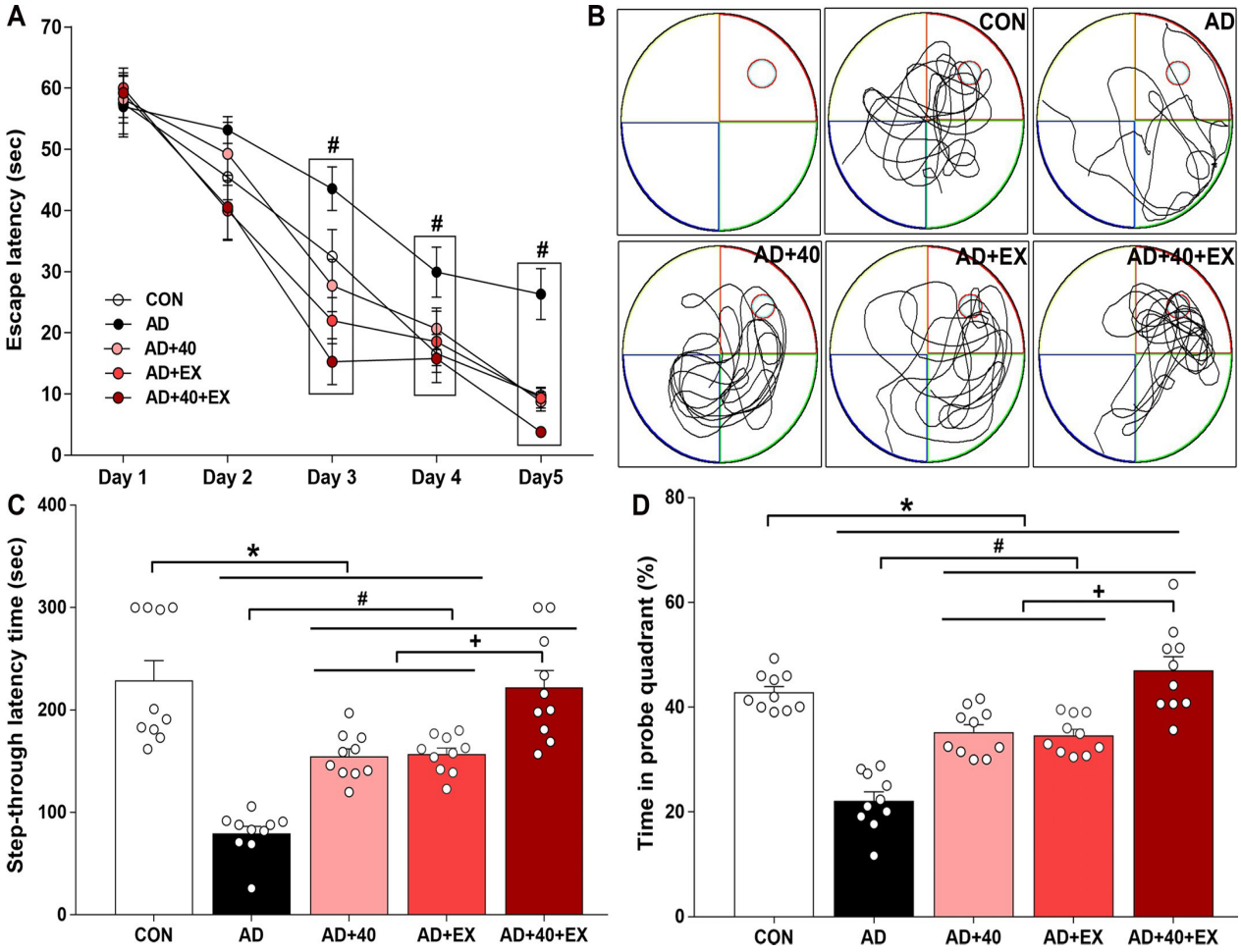

Figure 2. Effects of exercise under exposure to 40-Hz light flicker on spatial learning (*A*) and memory (*B*, *D*) and long-term memory (*C*) in the AD. The Morris water maze task was used to evaluate spatial learning and memory and step-through task was used for long-term memory. CON: nontransgenic, AD: 3xTg-AD, AD þ 40: 3xTg-AD, and 40-Hz light flickering AD þ EX: 3xTg-AD and exercise, AD þ 40 þ EX: 3xTg-AD and exercise with 40-Hz light flickering. Data are expressed as means ± SE. $^{*}P < 0.05$ compared with the CON group. #$P < 0.05$ compared with the AD group. þ $P < 0.05$ compared with the AD þ 40 þ EX group.

Effect of Exercise Exposure with 40-Hz Light Flicker on Akt, GSK3*β* , APP, Tau, and A*β* in the Hippocampus in Early 3xTg-AD

In the hippocampus, Akt, GSK3β, Tau, and APP protein expression changes were analyzed by Western blotting (Fig. 3). For comparison among groups, the value for the CON group was set to 1.0 and relative values for each treatment group were compared. Compared with the CON group, the t- Akt/p-Akt (*P*

< 0.001) and p-GSK3β/GSK3β ratios (P < 0.001) were lower and the t-Tau/p-Tau ratio (P < 0.001) and APP protein (P < 0.001) expression level were higher in the AD group. Akt and GSK3β levels were increased in 40-Hz light flicker group (t-Akt/p-Akt ratio: P = 0.037; p-GSK3β/GSK3β ratio: P = 0.033), exercise group (t-Akt/p-Akt ratio: P = 0.034; p-GSK3β/GSK3β ratio: p = 0.008), and the combination treatment group (t-Akt/p-Akt ratio: P < 0.001; p-GSK3β/GSK3β ratio: P < 0.001), and the combination treatment had a greater effect than that of single treatment with 40-Hz light flicker (t-Akt/p-Akt ratio: P = 0.022; p-GSK3β/GSK3β ratio: P = 0.007) or exercise (t-Akt/p-Akt ratio: P = 0.024; p-GSK3β/ GSK3β ratio: P = 0.029). Tau and APP levels were decreased in the 40-Hz light flicker group (t-tau/p-tau ratio, APP, P < 0.001, respectively) and exercise group (t-tau/p-tau ratio, APP, P < 0.001, respectively) and in the combination treatment group (t-tau/p-tau ratio, APP P < 0.001, respectively).

The combination treatment showed better results than those for the single treatment with 40-Hz light flicker (t-tau/ p-tau ratio, each APP P < 0.001) or exercise (t-tau/p-tau ratio, APP each P < 0.001). To identify Aβ-positive cells, CA1 of the hippocampus was analyzed by immunohistochemistry. In the CON group, Ab-positive cells were not found in CA1 of the hippocampus. Compared with the AD group, hippocampal CA1 Aβ-positive cells (P < 0.001) were decreased in the 40-Hz light flicker group, exercise group, and combination treatment group, and the effects for the combination treatment were greater than those for the single treatment of 40-Hz light flicker (P = 0.001) and exercise (P < 0.001). In particular, Akt/GSK3β/tau/APP protein expression levels improved to the level observed in the nontransgenic CON group.

Effect of Exercise Exposure with 40-Hz Light Flicker on Neuroinflammation and Proinflammatory Cytokines in the Hippocampus in Early 3xTg-AD

To evaluate neuroinflammation in the hippocampus, GFAP-positive astrocytes and Iba-1-positive microglial cells were analyzed by immunohistochemistry (Fig. 4). Compared with the CON group, neuroinflammation was increased in the hippocampal CA1 and DG in the AD group (GFAP and Iba-1: P < 0.001). Compared with the AD

group, GFAP and Iba-1 levels were lower in the 40-Hz light flicker group, exercise group, and combination treatment group [GFAP (P = 0.002) and Iba-1 (P = 0.001) from CA1, and GFAP (P < 0.001) and Iba-1 (P < 0.001) from DG]. In addition, the combined treatment with 40-Hz light flicker and exercise decreased these markers in the CA1 and DG of the hippocampus more substantially than the decreases in response to single treatments (GFAP and Iba-1: P < 0.001). Levels of proinflammatory cytokines in the hippocampus, i.e., TNF-α and IL-6, were analyzed by Western blotting. Levels in the CON group were set to 1.0 and used to determine relative values in each group. The expression levels of proinflammatory cytokines were higher in the AD group than in the CON group (TNF-α: P < 0.001; IL-6: P < 0.001). These levels were lower in the 40-Hz light flicker group (TNF-α: P = 0.003; IL-6: P = 0.004), exercise group (TNF-α: P = 0.008; IL-6: P < 0.001), and combination treatment group (TNF-α, IL-6: each P < 0.001) than in the AD groups. In addition, the combination treatment of 40-Hz light flicker and exercise resulted in greater decreases than either single treatment (40-Hz light flicker: TNF-α: P = 0.004, IL-6: P < 0.001; exercise: TNF-α, IL-6: both P = 0.001). Neuroinflammation and proinflammatory cytokine expression recovered to the levels in the nontransgenic CON group.

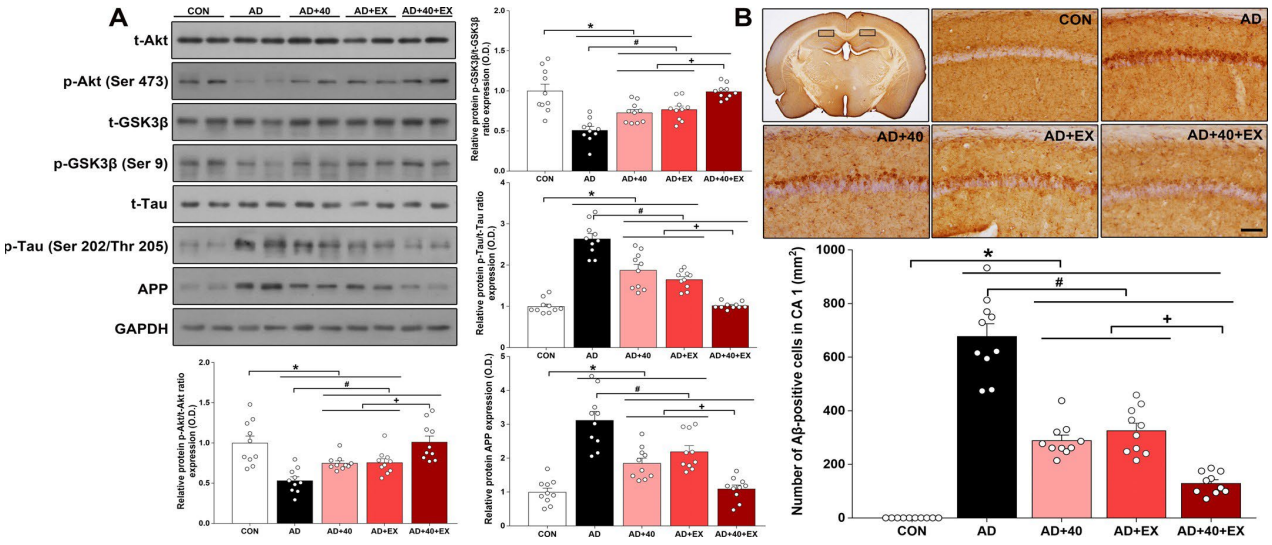

Figure 3. Effects of exercise under exposure to 40-Hz light flicker on the p-Akt/t-Akt, p-GSK3β/t-GSK3β and p-tau/t-tau ratios in the hippocampus (*A*) and Ab in hippocampal CA1 (*B*) of AD. Representative photomicrographs and data for Aβ-positive cells are shown. The scale bar represents 50 mm. CON: nontransgenic, AD: 3xTg-AD, AD + 40: 3xTg-AD, and 40-Hz light flickering AD + EX: 3xTg-AD and exercise, AD + 40 + EX: 3xTg-AD and exercise with 40-Hz light flickering. Data are expressed as means ± SE. $^{*}P < 0.05$ compared with the CON group. #$P < 0.05$ compared with the AD group. + $P < 0.05$ compared with the AD + 40 + EX group.

Effect of Exercise Exposure with 40-Hz Light Flicker on Mitochondrial Function and PTP Opening in the Hippocampus of Early 3xTg-AD

To determine mitochondrial function and PTP in the hippocampus, mitochondrial Ca^{2+} retention capacity, H_2O_2 emission, and levels of ANT1/2, VDAC1, and Cyp-D were evaluated (Fig. 5). In the hippocampus, the mitochondrial Ca^{2+} retention capacity was lower in the AD group than in the CON group ($P < 0.001$). It was higher in the 40-Hz light flicker group ($P = 0.015$), exercise group ($P = 0.006$), and combined treatment group ($P < 0.001$) than in the AD group. In addition, the increase in the Ca^{2+} retention capacity was greater for the combined treatment than for single treatments (40-Hz light flicker: $P = 0.006$; exercise: $P = 0.015$). To determine the mPTP opening sensitivity, the CON group of Ca^{2} þ retention in the CON group (set to 100%) was used as the baseline. Compared with the CON group, the mPTP opening sensitivity was lower in the AD group ($P < 0.001$) and higher in 40-Hz light flicker ($P = 0.040$), exercise ($P = 0.036$), and combined treatment groups ($P < 0.001$). In addition, the increase in sensitivity was greater for the combination treatment than for single treatments (40-Hz light flicker: $P = 0.041$; exercise: $P = 0.045$). Furthermore, mPTP- related membrane proteins were analyzed in isolated mitochondria. Mitochondrial membrane proteins, including ANT1/2, VDAC1, and Cyp-D, were more highly expressed in the AD group than in the CON group (all $P < 0.001$). Expression was suppressed in the 40-Hz light flicker group (ANT1/2: $P < 0.001$, VDAC1: $P = 0.001$, Cyp-D: $P = 0.001$), exercise group (all $P < 0.001$), and combination treatment group (all $P < 0.001$). Protein levels were lower for the combination treatment than for single treatments [40-Hz light flicker (ANT1/2: $P = 0.006$, VDAC1: $P = 0.002$, Cyp-D: $P = 0.003$); Exercise (ANT1/2: $P = 0.031$, VDAC1: $P = 0.034$, Cyp-D: $P = 0.014$)]. The mitochondrial H_2O_2 emission rate was calculated on *Complex I* substrate (glutamate þ malate; GM), *Complex 2* substrate (succinate; GMS), and a lipid substrate (glycerol-3 phosphate; GMSG3P). For the H_2O_2 emission rate, an ROS marker, there were no differences among groups on the *Complex 1* substrate. On the *Complex 2* substrate, compared with the CON group, the H_2O_2 emission rate was higher in

the AD group ($P = 0.001$) and was significantly lower in the combination treatment group ($P = 0.005$) but not in other treatment groups. Finally, for the lipid substrate, the H_2O_2 emission rate was also higher in the AD group than in the CON group ($P < 0.001$). The emission rate decreased in the 40-Hz light flicker group ($P = 0.001$), exercise group ($P = 0.007$), and combination treatment group ($P < 0.001$). The reduction in the emission rate was greater for the combination treatment than for each treatment group (40-Hz light flicker: $P = 0.031$, exercise: $P = 0.003$). The combination treatment was more effective in improving mitochondrial function and permeability of the hippocampus, with recovery to the levels observed in the nontransgenic CON group.

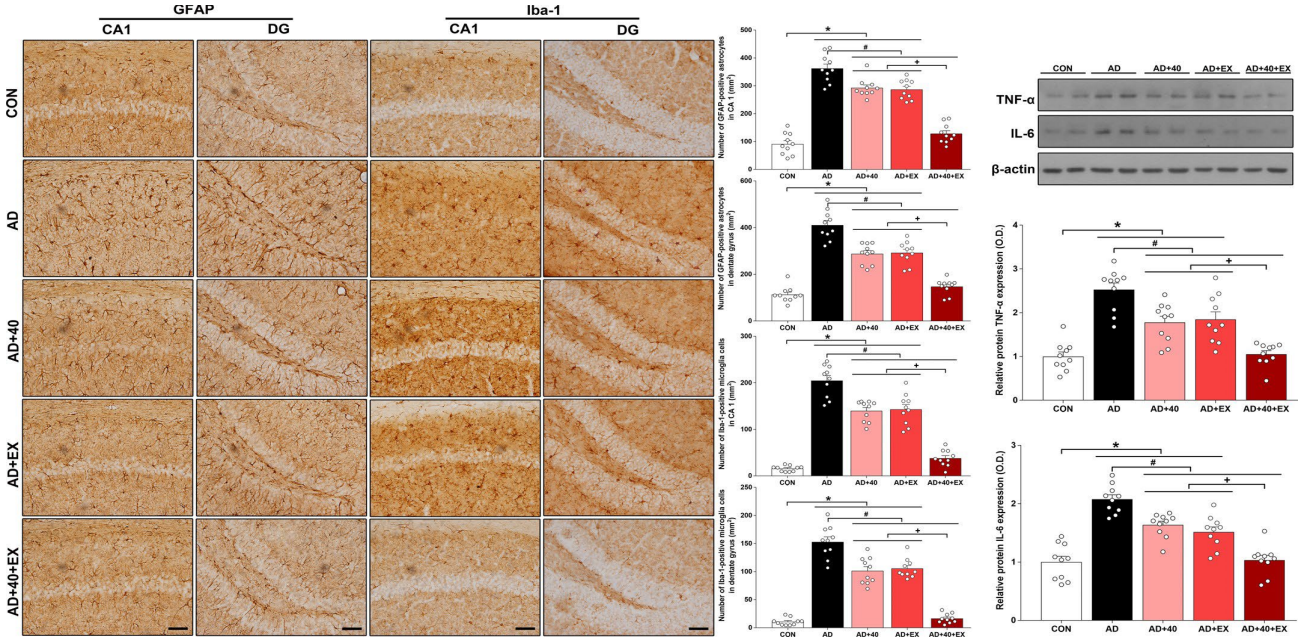

Figure 4. Effects of exercise under exposure to 40-Hz light flicker on neuroinflammation in the hippocampal CA1 and DG and proinflammatory cytokines in the hippocampus of AD. Representative photomicrographs and data for GFAP-positive astrocytes and Iba-1-positive microglial cells are shown. The scale bar represents 50 mm. CON: nontransgenic, AD: 3xTg-AD, AD + 40: 3xTg-AD, and 40-Hz light flickering AD + EX: 3xTg-AD and exercise, AD + 40 +EX: 3xTg-AD and exercise with 40-Hz light flickering. Data are expressed as means ± SE. $^{*}P < 0.05$ compared with the CON group. $\#P < 0.05$ compared with the AD group. + $P < 0.05$ compared with the AD + 40 þ EX group.

Effect of Exercise Exposure with 40-Hz Light Flicker on Apoptosis and Cell Death in the Hippocampus in Early 3xTg-AD

Changes in apoptosis-related proteins in the hippocampus, including Bax, Bcl-2, cytochrome c, and cleaved cas-pase-3, were analyzed, and TUNEL-

positive cells were analyzed to determine cell death (Fig. 6). Values in the CON group value were set to 1.0 and used to obtain relative values for comparisons among groups. Compared with the CON group, Bax, cytochrome c, and cleaved caspase-3 levels were higher and Bcl-2 levels were lower in the AD group (all $P < 0.001$). The expression levels of Bax, cytochrome c, and cleaved caspase-3 decreased in the individual treatment groups [40-Hz light flicker group (Bax: $P < 0.001$, cytochrome c: $P = 0.002$, caspase-3: $P < 0.001$), exercise group (Bax: $P < 0.001$, cytochrome c: $P = 0.007$, caspase-3: $P < 0.001$), and combined treatment group (all $P < 0.001$)], and Bcl-2 levels increased in the 40-Hz light flicker group ($P = 0.042$), exercise group ($P = 0.039$), and combined treatment group ($P < 0.001$). In addition, the decrease in apoptosis was greater in the combination treatment group than in each single treatment group (40-Hz light flicker: Bax: $P = 0.028$, Bcl-2: $P = 0.001$, cytochrome c: $P = 0.042$, caspase-3: $P = 0.002$; exercise: 40-Hz light flicker: Bax: $P = 0.027$, Bcl-2: $P = 0.002$, cytochrome c: $P = 0.016$, caspase-3: $P = 0.044$). TUNEL-positive cells were analyzed to determine final cell death rates in the hippocampus. In the hippocampus, the number of TUNEL-positive cells was higher in the AD group ($P < 0.001$) and lower in the 40-Hz light flicker group ($P < 0.001$), exercise group ($P = 0.002$), and combined treatment group ($P < 0.001$) than in the CON group. In addition, cell death was greater in the combination treatment group than in the single treatment groups (all $P < 0.001$). Therefore, simultaneous treatment was more effective in inhibiting hippocampal apoptosis and cell death, with recovery to levels observed in the nontransgenic CON group.

Effect of Exercise Exposure with 40-Hz Light Flicker on BDNF, Synaptophysin, and PSD95 in the Hippocampus in Early 3xTg-AD

The expression levels of the synaptic proteins BDNF, PSD 95 and synaptophysin were investigated in the hippocampus (Fig. 7). Levels in the CON group were set to 1.0 to obtain relative values in each group. Compared with the CON group, protein expression levels were decreased in the AD group (all $P < 0.001$) but were higher in each treatment group, including the 40-Hz light flicker

group (BDNF: $P = 0.032$, synaptophysin: $P = 0.005$, PSD95: $P = 0.046$), exercise group (BDNF: $P = 0.015$, synaptophysin: $P = 0.001$, PSD95: $P < 0.001$), and combination treatment group (all $P < 0.001$). The increases in expression were higher in the combination treatment group than in single treatment groups (40-Hz light flicker: all $P < 0.001$, exercise: BDNF and synaptophysin: $P < 0.001$, PSD95: $P = 0.001$). Accordingly, the combined treatment was more effective in increasing the expression of synapse- related proteins; in particular, BDNF levels were equal to or better than those in the nontransgenic CON group.

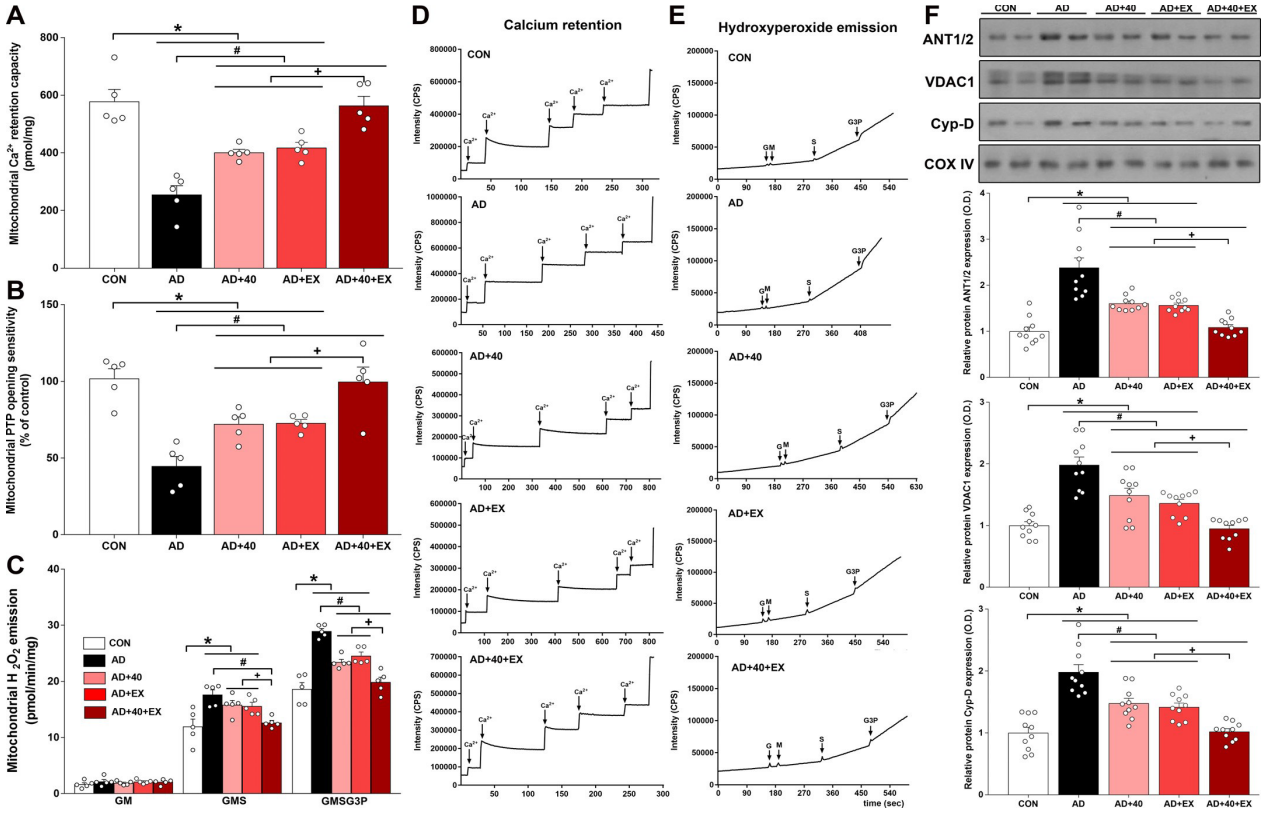

Figure 5. Effects of exercise under exposure to 40-Hz light flicker on mitochondrial Ca^{2+} retention (*A*), mPTP (*B*), H_2O_2 emission (*C*), and mPTP-related protein expression (*F*) in the hippocampus of AD. The total mitochondrial Ca^{2+} retention capacity before PTP opening (i.e., release of Ca^{2+}) was deter- mined. Ca^{2+}↓ indicates Ca^{2+} infusion in calcium retention (*D*). G↓ indicates glutamate infusion; M↓ indicates malate infusion; S↓, succinate infusion; G3P↓ indicates glycerol-3-phosphate infusion in hydroxyperoxide emission (*E*). CON: nontransgenic, AD: 3xTg-AD, AD þ 40: 3xTg-AD, and 40-Hz light flickering AD + EX: 3xTg-AD and exercise, AD + 40 þ EX: 3xTg-AD and exercise with 40-Hz light flickering. Data are expressed as means ± SE. *P <0.05 compared with the CON group. #$P < 0.05$ compared with the AD group. + $P < 0.05$ compared with the AD þ 40 þ EX group. PTP, permeability transition pore.

Effect of Exercise Exposure with 40-Hz Light Flicker on Cell Differentiation and Neurogenesis in the Hippocampal DG of Early 3xTg-AD

DCX-positive cells and NeuN/BrdU-positive cells were evaluated to investigate cell differentiation and neurogenesis in the hippocampus (Fig. 8). The frequencies of hippocampal DCX-positive cells and NeuN/BrdU-positive cells were lower in the AD group than in the CON group (both $P < 0.001$) but were increased in the 40-Hz light flicker group (DCX: $P < 0.001$, NeuN/BrdU: $P = 0.004$), exercise group, and combination treatment group (both $P < 0.001$). The increases in DCX-positive cells ($P < 0.001$) and NeuN/BrdU- positive cells (40-Hz light flicker: $P < 0.001$, exercise: $P = 0.001$) were greater with the combined treatment than with single treatments. Therefore, the combination of the two treatments increased cell differentiation and neurogenesis in the hippocampus, with recovery to the levels observed in the nontransgenic CON group.

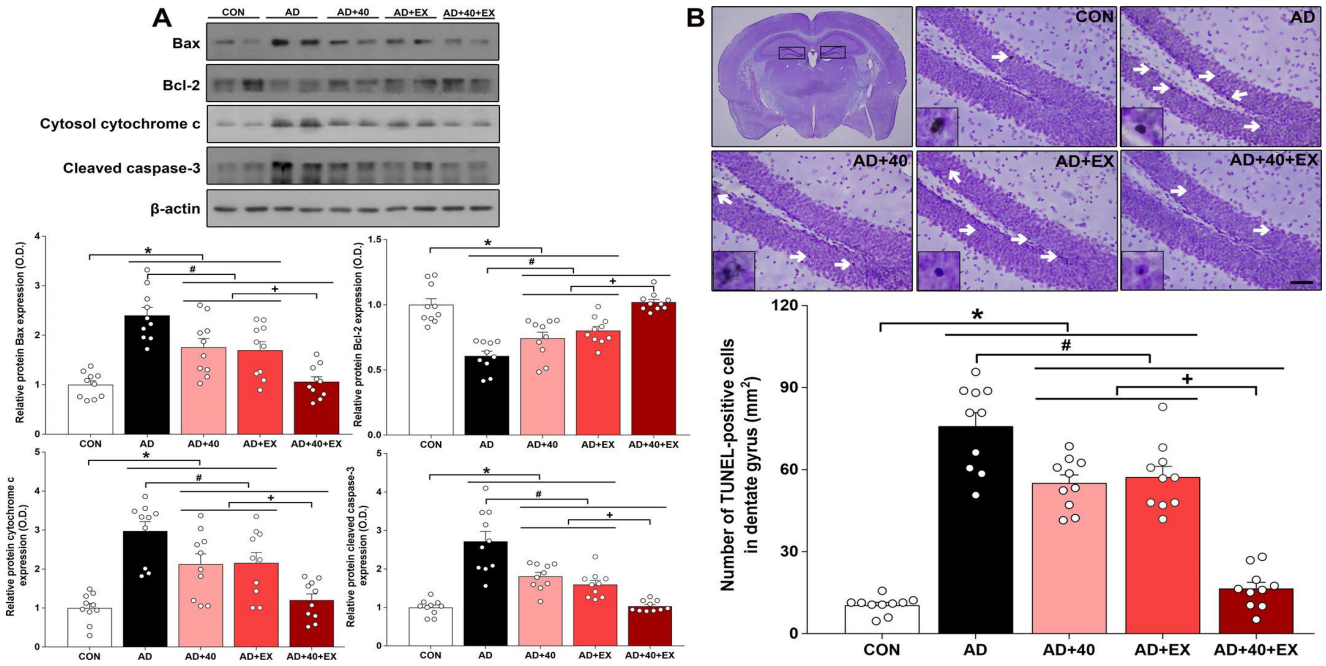

Figure 6. Effects of exercise under exposure to 40-Hz light flicker on apoptosis (*A*) and cell death (*B*) in the hippocampus of AD. Representative photomicrographs and data for TUNEL-positive cells are shown. The scale bar represents 50 mm. CON: nontransgenic, AD: 3xTg-AD, AD + 40: 3xTg-AD, and 40-Hz light flickering AD + EX: 3xTg-AD and exercise, AD + 40 + EX: 3xTg-AD and exercise with 40-Hz light flickering. Data are expressed as means ± SE. $^{*}P < 0.05$ compared with the CON group. $\#P < 0.05$ compared with the AD group. $+ P < 0.05$ compared with the AD + 40 + EX group.

DISCUSSION

AD, the primary cause of dementia, begins in the temporal lobe and encroaches on all areas of the brain. Since the hippocampus is located in the temporal lobe, memory impairment is a common symptom of AD. Similar to many diseases, treatment in the early stage of AD is critical for better treatment effects. Previous studies have shown that 3xTg-AD mice begin to develop deficiencies in short-term memory, long-term memory, and spatial learning and memory at 4 mo (24), 6 mo, and 6.5 mo of age (25, 26). Although these findings provide insights into the early stages of various cognitive deficiencies, they do not provide information about how these variables change over time (25). Consistent with previous studies, we found impairments in spatial learning and memory, and long-term memory in the AD group. These AD-related cognitive dysfunctions align with the amyloid cascade hypothesis, in which the onset of dis- ease could be characterized by changes in Ab, followed by a series of events, including the accumulation of toxic forms of tau, which ultimately leads to apoptosis (1). Accordingly, the purpose of this study was to examine the effects of exercise combined with 40-Hz light flickering on cognitive function in an early stage (5 mo) 3xTg AD mouse model. The main findings of this study were that *1*) exercise combined with 40-Hz light flickering could reduce AD risk factors, such as Ab and tau and *2*) exercise combined with 40-Hz light flickering could improve mitochondrial function and neuroplasticity in the hippocampus in the early stage of cognitive dysfunctional a 3xTg AD mouse model. Our findings may provide clinical insights into the favorable effects of exercise combined with 40-Hz light flickering as a potential treatment to prevent and slow the disease progression of AD in all stages.

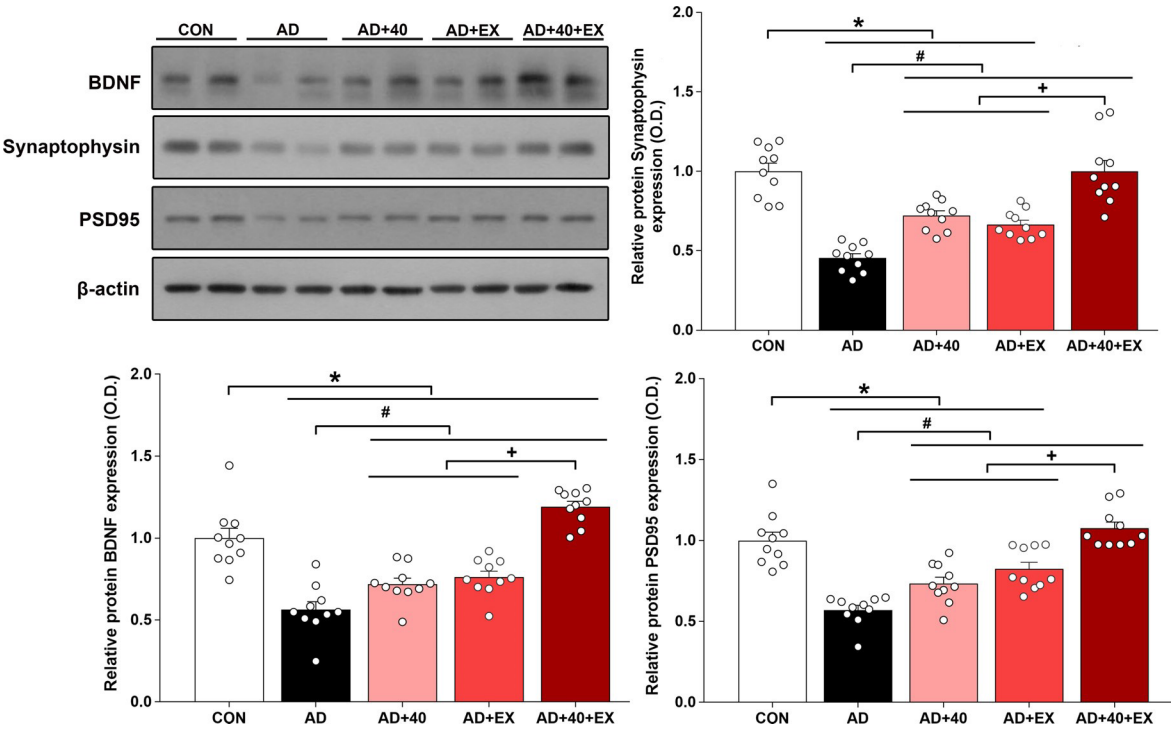

Figure 7. Effects of exercise under exposure to 40-Hz light flicker on BDNF, synaptophysin, and PSD95 in the hippocampus of AD. CON: nontransgenic, AD: 3xTg-AD, AD + 40: 3xTg-AD, and 40-Hz light flickering AD + EX: 3xTg-AD and exercise, AD + 40 + EX: 3xTg-AD and exercise with 40-Hz light flickering. Data are expressed as means ± SE. $^{*}P < 0.05$ compared with the CON group. $\#P < 0.05$ compared with the AD group. þ $P < 0.05$ compared with the AD + 40 þ EX group. BDNF, brain-derived neurotrophic factor.

Amyloid plaque deposition begins in the neocortex several years before the onset of symptoms and gradually spreads to the hippocampus, diencephalon, striatum, brainstem, and finally the cerebellum (27). In 3xTg mice, extensive neurofibrillary tangles develop, which first appear in pyramidal neuron of hippocampal CA1 subfield and then in the cortex(28). Brains of patients with AD showed a significant neuronal decrease compared with normal brains in the CA1 of the hippocampus (29). In the brains of human and animal models, the expression of APP, presenilin mutations, and plaques, which are related to AD, is not only associated with synaptic loss, but also with a deficiency of memory and synaptic plasticity (30–33). Pathological forms of Aβ and tau, as well as glia-mediated neuroinflammation, play critical roles in synaptotoxicity (34). Microglial cells and astrocytes exhibit changes in gene expression, morphology, and secretion in response to toxic stimuli in the brain, and these alterations affect other cells, including neurons (1). The activation of microglial

cells and astrocytes in the early stage of AD results in microgliosis, astrogliosis, impairments in amyloid and tau removal, neurotoxin release, and proinflammatory cytokine release (35–39). Previous studies have reported that the frequencies of GFAP-positive astrocytes and Iba-1 micro-glial cells are increased in the 3xTg-AD hippocampus at 6 and 10 mo (40–42). Microglial cells and astrocytes associated with amyloids secrete proinflammatory cytokines, such as IL-1b, IL-6, and TNF-α (43). In various animal models of AD, the entire brain, including the hippocampus and hypothalamus, shows increases in IL-6 and TNF-α at the mRNA and protein levels (44–46). In particular, elevated IL-6 leads to the release of a cascade of proinflammatory cytokines by microglia and astrocytes (47). Consistent with previous results, in this study, tau hyperphosphorylation and APP expression were significantly higher, p-Akt and p-GSK3β in the hippocampus were significantly lower, and Aβ-positive cells in CA1 were significantly higher in the AD group than in the control group. These results suggested that the dysregulation of Tau and Aβ increased the expression of TNF-α and IL-6 by activating astrocyte and microglia in the hippocampus. As such, Aβ, tau, and phosphorylation are associated with increases in proinflammatory cytokine levels via the activation of microglia and astrocytes, which contribute to Ca^{2+} dysregulation (48), ROS (43), and cell death (49). In addition, mitochondria provide an important buffer for regulating calcium concentrations during signaling, which is particularly important for excitatory cells, such as neurons (50).

Mitochondrial dysfunction related to Aβ, such as ROS production (51, 52) and the disruption of calcium homeostasis (53), is frequently observed in patients with AD and in animal models. The mPTP is associated with factors of Aβ-induced mitochondrial dysfunction, such as disturbances of intracellular calcium regulation, ROS, and the release of proapoptotic factors (54). In previous studies, mitochondria from mice with AD had much lower calcium handling capacities than nontransgenic mouse mitochondria, and the impaired Ca^{2+} uptake capacity, which started at 6 mo, kept decreasing gradually. This decreased Ca^{2+} retention capacity increased the expression of cyclophilin D (cyp-D), a mitochondrial matrix component, and mPTP components, such as voltage-dependent anion channel 1 (VDAC1) of the outer

membrane (55, 56). Adenine nucleotide trans- locator (ANT), a component of the inner membrane, binds to cyp-D and interacts with Aβ. ANT strongly interacts with Aβ to change mPTP regulation and is related to mitochondrial dysfunction (54). In addition, H_2O_2 is an important ROS that induces oxidative damage, and an increase in mitochondrial H_2O_2 is significantly associated with the onset of AD (55, 58). Mitochondrial dysfunction, including increases in mPTP and ROS, can induce increased apoptosis. In addition, increased levels of cyp-D, VDAC1, and ANT increase apoptosis (55–57). Furthermore, H_2O_2 penetrates all tissue compartments, triggers oxidative toxicity, and eventually induces apoptosis (59). Therefore, mitochondria play an important role in regulating the fundamental processes of neuroplasticity (60) and are also associated with changes in synaptic plasticity (59).

Mitochondrial dysfunction, caused by Aβ, may be related to neuroplasticity changes. Synapse-related proteins, such as BDNF, PSD95, synaptophysin (in the hippocampus in the early stage), DCX, and neurogenesis are decreased in various AD animal models (61–66). In this study, the Ca^{2+} retention capacity was significantly lower and H_2O_2 emission was higher in hippocampal mitochondria in the AD group compared with the control group. In addition, mPTP-related proteins were overexpressed, such as Bax, a proapoptotic factor, cytochrome c, and cleaved caspase-3, and decreases in Bcl-2, an anti-apoptotic factor, may increase cell death. In addition, synapse-related proteins, such as BDNF, PSD95, and synaptophysin, as well as DCX and neurogenesis decreased. In patients with AD, decreased levels of BDNF in the blood and brain and impaired neurogenesis have been observed in the early stages of the disease along with decreased cognitive function (67–69). There is a positive correlation between the BDNF concentration and cognitive function (70). As such, it has been accepted that Ab production or aggregation and tau phosphorylation, via direct or indirect pathways, affects neuroinflammation, mitochondrial function, apoptosis, and synapses in various brain regions, including the hippocampus, leading to cognitive decline.

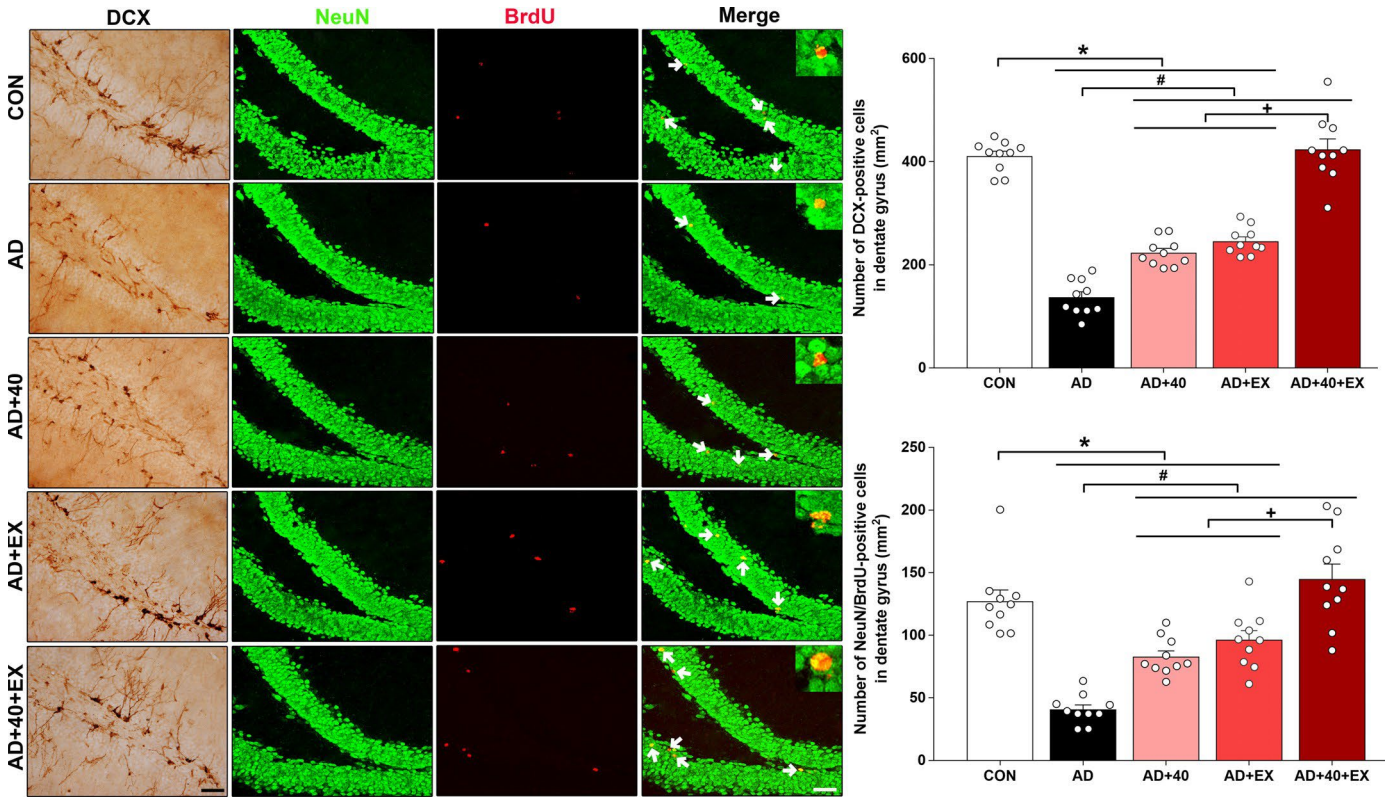

Figure 8. Effects of exercise under exposure to 40-Hz light flicker on cell differentiation and neurogenesis in the hippocampal dentate gyrus of AD. Representative photomicrographs and data for DCX- and NeuN/BrdU-positive cells are shown. The scale bar represents 50 mm. CON: nontransgenic, AD: 3xTg-AD, AD + 40: 3xTg-AD, and 40-Hz light flickering AD + EX: 3xTg-AD and exercise, AD + 40 + EX: 3xTg-AD and exercise with 40-Hz light flickering. Data are expressed as means ± SE. $^{*}P < 0.05$ compared with the CON group. #$P < 0.05$ compared with the AD group. + $P < 0.05$ compared with the AD + 40 + EX group. DCX, doublecortin.

Altered gamma oscillations have been observed in several brain regions in various neurological and psychological disorders, including a decrease of spontaneous gamma synchronization in patients with AD and a decrease in gamma power in several AD mouse models (71–74). Although gamma oscillations could not be measured in this study, they are associated with functional decline in AD, as established in an APP/PS1 model of AD (75). Gamma oscillations in the hippocampus are degraded according to the concentration and accumulation of Aβ (76) and damaged mitochondrial function abolishes gamma oscillations in the hippocampal network (77). In a transgenic mouse model of AD, theta-gamma coupling was found to be defective in the subiculum, the major output area of the hippocampus (78). Recent work has shown that 40-Hz light flicker stimulation, a noninvasive treatment method,

reduces Aβ and phosphorylated tau in various AD animal models by entraining gamma oscillations through the visual cortex. This 40-Hz light flicker stimulation may improve spatial learning and memory by reducing the progression of the degenerative state of neurons, improving synaptic function, enhancing neuronal protective factors, reducing DNA damage, and reducing the inflammatory response of microglia (19, 20, 79).

Furthermore, 40-Hz auditory stimulation boosts hippocampal function by gamma entrainment and combined visual and auditory stimulation, which improves cognitive function by reducing amyloid accumulation to a greater degree (21). In this study, Aβ and phosphorylated tau in the hippocampus were significantly attenuated in the 40-Hz light flicker group, as were Iba-1-positive microglial cells and GFAP-positive astrocytes. Long-term 40-Hz light flicker stimulation through the visual cortex stabilized gamma oscillations and alleviated Aβ, tau, and inflammatory responses in the hippocampus.

Exercise interventions have a positive effect on brain function and can be a useful modality to reduce the incidence of dementia and AD (80). Physical exercise has been shown to decrease Aβ and tau levels and increase memory. Furthermore, high-intensity exercise has been suggested to be an effective modality to decrease Aβ in the plasma and brain of patients with AD (81–83). Therefore, exercise is considered a powerful tool to prevent neuroinflammation and the decline of cognitive function (17).

Liu et al. (83) showed that exercise increases the expression of Akt/GSK3β pathway members in the 3xTg-AD model, decreases Ab deposition, and decreases Iba-1-positive micro- glial cells and GFAP-positive astrocytes in the hippocampal DG. Exercise at the early stage of AD has a protective effect on cognitive function by reducing Aβ plaques and GFAP-positive astrocytes in the hippocampus and increasing neurogenesis (42). Exercise has anti-inflammatory effects, which inhibits proinflammatory cytokines, such as TNF-α, IL-6, and IL1β, in the tau-transgenic hippocampus (84).

In this study, the AD exercise group showed increases in Akt/GSK3β pathway expression, decreases in tau and Ab, and decreases in excessive Iba-

1-positive microglial cells and GFAP-positive astrocytes, as well as decreases in TNF-α and IL-6 expression in the hippocampus. Exercise improves the antioxidant defense system, which reduces ROS levels, and adaptations to long-term exercise directly decrease ROS production, which reduces oxidative damage (17) through the improvement of mitochondrial function. Previous studies suggested that exercise training has a protective effect against mitochondrial degeneration and cell death in the hippocampus, cortex, and cerebellum (85, 86). Furthermore, exercise inhibits the overexpression of membrane-related proteins, which can increase the blood–brain barrier thickness, concentrations of permeability markers, such as ANT1/ 2, Cyp-D, and VDAC1, and ROS markers, such as H_2O_2 (86). Therefore, in an AD transgenic and systemic model, Bax, cytochrome c, caspase 3, and caspase 9 levels are decreased, and Bcl-2 levels are increased after exercise (85, 86, 88). Brain mitochondrial function increases in a BDNF concentration-dependent manner (87), and BDNF expression increases in response to exercise (90, 91). Neurotrophin is associated with learning, memory, neuronal activity, and plastic responses (92, 93). Decreases in synapse-related proteins, such as PSD95 and synaptophysin, in the hippocampus, in the early stage of AD, are also increased by exercise (94, 95). Exercise, especially through increased neurogenesis, with decreased Aβ in the AD hippocampus and increased BDNF, improves cognitive function (96).

We found that the exercise group exhibited improved mitochondrial function with increased Ca^{2+} retention capacity, decreased mPTP proteins, including ANT1/2, VDAC1, and Cyp- D, decreased H_2O_2 emissions in the hippocampal mitochondria, reduced cell death via decreased Bax, cytochrome c, and caspase-3, and increased Bcl-2. In addition, BDNF, synaptophysin, PSD95, and neurogenesis were increased. Therefore, in early AD, exercise seems to have a protective effect on cognitive function by improving the neuroplasticity of the mitochondria and hippocampus.

Under the induction of a noninvasive 40-Hz light flicker environment, exercise seemed to have a greater effect. A limitation of this study was the

inability to analyze gamma oscillations. However, under an environment where gamma oscillations are entrained through 40-Hz light flicker by the visual cortex that improves Aβ and tau pathology by inducing a variety of positive cellular changes, exercise may result in the stimulation of various brain regions via various myokines secreted from the muscles.

We previously reported that the combination of exercise with 40-Hz light flicker could improve cognitive function in the end stage (12 mo) of a 3xTg-AD mouse model, and fortunately, we have found similar beneficial effects in the early stage (5 mo) of a 3xTg-AD mouse model. Therefore, we conclude that the combination of exercise with 40-Hz light flicker, both of which are nonpharmacological and noninvasive methods, efficiently improved mitochondrial function and neuroplasticity by reducing accumulation of Aβ and tau, which are closely linked to AD. This intervention may be an effective lifestyle modification and useful practice for preventing cognitive decline by suppressing the expression of Aβ and tau, neuroinflammation, and mitochondrial function and by protecting against deficiencies in neuroplasticity of the hippocampus in the early stage of AD. Future studies are warranted to investigate a wider range of parameters and clinical applications.

GRANTS

This work was supported by the Ministry of Education of the Republic of Korea and the National Research Foundation of Korea (NRF-2017S1A5B5A02025250).

DISCLOSURES

No conflicts of interest, financial or otherwise, are declared by the author.

AUTHOR CONTRIBUTIONS

S-S.P. and T-W.K. conceived and designed research; S-S.P. and T-W.K. performed experiments; T-W.K. analyzed data; S-S.P., H-S.P., C-J.K., S-S.B., S-Y.P., and T-W.K. interpreted results of experiments; T-W.K. prepared figures; H-S.P., M-K.K., and T-W.K. drafted manuscript; C-J.K., S-S.B., S-Y.P., C.A., M-K.K., and I-R.P. edited and revised

manuscript; T-W.K. approved final version of manuscript.

REFERENCES

1. Henstridge CM, Hyman BT, Spires-Jones LT. Beyond the neuron–cellular interactions early in Alzheimer's disease pathogenesis. *Nat Rev Neurosci* 20: 94–108, 2019. doi:10.1038/s41583-018-0113-1.

2. Hardy JA, Higgins GA. Alzheimer's disease: the amyloid cascade hypothesis. *Science* 256: 184–185, 1992. doi:10.1126/science.1566067.

3. Karran E, De Strooper B. The amyloid cascade hypothesis: are we poised for success or failure? *J. Neurochem1* 39: 237–252, 2016. doi:10.1111/jnc.13632.

4. Takahashi RH, Capetillo-Zarate E, Lin MT, Milner TA, Gouras GK. Co-occurrence of Alzheimer's disease ß-amyloid and pathologies at synapses. *Neurobiol Aging* 31: 1145–1152, 2010. doi:10.1016/j.neurobiolaging.2008.07.021.

5. Colom-Cadena M, Spires-Jones T, Zetterberg H, Blennow K, Caggiano A, Dekosky ST, Fillit H, Harrison JE, Schneider LS, Scheltens P, de Haan W, Grundman M, van Dyck CH, Izzo NJ, Catalano SM; Synaptic Health Endpoints Working Group. The clinical promise of biomarkers of synapse damage or loss in Alzheimer's disease. *Alzheimers Res Ther* 12: 21, 2020. doi:10.1186/s13195-020-00588-4.

6. Heneka MT, O'Banion MK, Terwel D, Kummer MP. Neuroinflammatory processes in Alzheimer's disease. *J Neural Transm (Vienna)* 117: 919–947, 2010. doi:10.1007/s00702-010-0438-z.

7. Grimaldi A, Brighi C, Peruzzi G, Ragozzino D, Bonanni V, Limatola C, Ruocco G, Di Angelantonio S. Inflammation, neurodegeneration and protein aggregation in the retina as ocular biomarkers for Alzheimer's disease in the 3xTg-AD mouse model. *Cell Death Dis* 9: 685, 2018. doi:10.1038/s41419-018-0740-5.

8. Zhao J, O'Connor T, Vassar R. The contribution of activated astrocytes to Ab production: implications for Alzheimer's disease pathogenesis. *J Neuroinflammation* 8: 150, 2011. doi:10.1186/1742-2094-8-150.

9. McGeer PL, McGeer EG. The inflammatory response system of brain: implications for therapy of Alzheimer and other neurodegenerative diseases. *Brain Res Brain Res Rev* 21: 195–218, 1995. doi:10.1016/0165-0173(95)00011-9.

10. Hoekstra JG, Hipp MJ, Montine TJ, Kennedy SR. Mitochondrial DNA mutations increase in early stage Alzheimer disease and are inconsistent with oxidative damage. *Ann Neurol* 80: 301–306, 2016. doi:10.1002/ana.24709.

11. Hauptmann S, Scherping I, Drose S, Brandt U, Schulz KL, Jendrach M, Leuner K, Eckert A, Muller WE. Mitochondrial dysfunction: an early event in Alzheimer pathology accumulates with age in AD transgenic mice. *Neurobiol Aging* 30: 1574–1586, 2009. doi:10.1016/j.neurobiolaging.2007.12.005.

12. Reddy PH. Amyloid b, mitochondrial structural and functional dynamics in Alzheimer's disease. *Exp Neurol* 218: 286–292, 2009. doi:10.1016/j.expneurol.2009.03.042.

13. Swerdlow RH, Khan SM. The Alzheimer's disease mitochondrial cascade hypothesis: an update. *Exp Neurol* 218: 308–315, 2009. doi:10.1016/j.expneurol.2009.01.011.

14. Aliev G, Palacios HH, Walrafen B, Lipsitt AE, Obrenovich ME, Morales L. Brain mitochondria as a primary target in the development of treatment strategies for Alzheimer disease. *Int J Biochem Cell Biol* 41: 1989–2004, 2009. doi:10.1016/j.biocel.2009.03.015.

15. Mancuso M, Coppede F, Murri L, Siciliano G. Mitochondrial cascade hypothesis of Alzheimer's disease: myth or reality? *Antioxid Redox Signal* 9: 1631–1646, 2007. doi:10.1089/ars.2007.1761.

16. Swerdlow RH, Khan SM. A “mitochondrial cascade hypothesis” for sporadic Alzheimer's disease. *Med Hypotheses* 63: 8–20, 2004. doi:10.1016/j.mehy.2003.12.045.

17. Geda YE, Roberts RO, Knopman DS, Christianson TJH, Pankratz VS, Ivnik RJ, Boeve BF, Tangalos EG, Petersen RC, Rocca WA. Physical exercise, aging, and mild cognitive impairment: a population-based study. *Arch Neurol* 67: 80–86, 2010. doi:10.1001/archneurol.2009.297.

18. Radak Z, Hart N, Sarga L, Koltai E, Atalay M, Ohno H, Boldogh I. Exercise plays a preventive role against Alzheimer's disease. *J Alzheimers Dis* 20: 777–783, 2010. doi:10.3233/JAD-2010-091531.

19. Iaccarino HF, Singer AC, Martorell AJ, Rudenko A, Gao F, Gillingham T, Mathys H, Seo J, Kritskiy O, Abdurrob F, Adaikkan C, Canter RG, Rueda R, Brown EN,

Boyden ES, Tsai LH. c frequency entrainment attenuates amyloid load and modifies microglia. *Nature* 540: 230–235, 2016. doi:10.1038/nature20587.

20. Singer AC, Martorell AJ, Douglas JM, Abdurrob F, Attokaren MK, Tipton J, Mathys H, Adaikkan C, Tsai LH. Noninvasive 40-Hz light flicker to recruit microglia and reduce amyloid b load. *Nat Protoc* 13: 1850–1868, 2018. doi:10.1038/s41596-018-0021-x.

21. Martorell AJ, Paulson AL, Suk HJ, Abdurrob F, Drummond GT, Guan W, Young JZ, Kim DNW, Kritskiy O, Barker SJ, Mangena V, Prience SM, Brown EN, Chung K, Boyden ES, Singer AC, Tsai LH. Multi-sensory gamma stimulation ameliorates Alzheimer's-associated pathology and improves cognition. *Cell* 177: 256–271, 2019. doi:10.1016/j.cell.2019.02.014.

22. Ferreira AC. Castellano JM. Leaving the lights on using gamma entrainment to protect against neurodegeneration. *Neuron* 120: 901–902, 2019. doi:10.1016/j.neuron.2019.05.020.

23. Billings LM, Oddo S, Green KN, McGaugh JL, LaFerla FM. Intraneuronal Ab causes the onset of early Alzheimer's disease- related cognitive deficits in transgenic mice. *Neuron* 45: 675–688, 2005. doi:10.1016/j.neuron.2005.01.040.

24. Clinton LK, Billings LM, Green KN, Caccamo A, Ngo J, Oddo S, McGaugh JL, LaFerla FM. Age-dependent sexual dimorphism in cognition and stress response in the 3xTg-AD mice. *Neurobiol Dis* 28: 76–82, 2007. doi:10.1016/j.nbd.2007.06.013.

25. Stover KR, Campbell MA, Van Winssen CM, Brown RE. Early detection of cognitive deficits in the 3xTg-AD mouse model of Alzheimer's disease. *Behav Brain Res* 289: 29–38, 2015. doi:10.1016/j.bbr.2015.04.012.

26. Thal DR, Ru€b U, Orantes M, Braak H. Phases of A b-deposition in the human brain and its relevance for the development of AD. *Neurology* 58: 1791–1800, 2002. doi:10.1212/WNL.58.12.1791.

27. Koffie RM, Hashimoto T, Tai HC, Kay KR, Serrano-Pozo A, Joyner D, Hou S, Kopeikina KJ, Frosch MP, Lee VM, Holtzman DM, Hyman BT, Spires-Jones TL. Apolipoprotein E4 effects in Alzheimer's disease are mediated by synaptotoxic oligomeric amyloid-b. *Brain* 135: 2155–2168, 2012. doi:10.1093/brain/aws127.

28. Oddo S, Caccamo A, Shepherd JD, Murphy MP, Golde TE, Kayed R, Metherate R, Mattson MP, Akbari Y, LaFerla FM. Triple-trans- genic model of Alzheimer's

disease with plaques and tangles: intra- cellular A b and synaptic dysfunction. *Neuron 31* 39: 409–421, 2003. doi:10.1016/s0896-6273(03)00434-3.

29. West MJ, Kawas CH, Stewart WF, Rudow GL, Troncoso JC. Hippocampal neurons in pre-clinical Alzheimer's disease. *Neurobiol Aging* 25: 1205–1212, 2004. doi:10.1016/j.neurobiolaging.2003.12.005.

30. Jackson RJ, Rudinskiy N, Herrmann AG, Croft S, Kim JM, Petrova V, Ramos-Rodriguez JJ, Pitstick R, Wegmann S, Garcia-Alloza M, Carlson GA, Hyman BT, Spires-Jones TL. Human tau increases amyloid b plaque size but not amyloid b-mediated synapse loss in a novel mouse model of Alzheimer's disease. *Eur J Neurosci* 44: 3056–3066, 2016. doi:10.1111/ejn.13442.

31. Ashe KH, Zahs KR. Probing the biology of Alzheimer's disease in mice. *Neuron* 66: 631–645, 2010. doi:10.1016/j.neuron.2010.04.031.

32. Sasaguri H, Nilsson P, Hashimoto S, Nagata K, Saito T, Strooper BD, Hardy J, Vassar R, Winblad B, Saido TC. APP mouse models for Alzheimer's disease preclinical studies. *EMBO J* 36: 2473–2487, 2017. doi:10.15252/embj.201797397.

33. de Wilde MC, Overk CR, Sijben JW, Masliah E. Meta-analysis of synaptic pathology in Alzheimer's disease reveals selective molecular vesicular machinery vulnerability. *Alzheimers Dement* 12: 633– 644, 2016. doi:10.1016/j.jalz.2015.12.005.

34. Heneka MT, Carson MJ, El Khoury J, Khoury JE, Landreth GE, Brosseron F, Feinstein DL, et al. Neuroinflammation in Alzheimer's disease. *Lancet Neurol* 14: 388–405, 2015. doi:10.1016/S1474-4422(15)70016-5.

35. Hickman S, Izzy S, Sen P, Morsett L, El Khoury J. Microglia in neurodegeneration. *Nat Neurosci* 21: 1359–1369, 2018. doi:10.1038/ s41593-018-0242-x.

36. Heppner FL, Ransohoff RM, Becher B. Immune attack: the role of inflammation in Alzheimer disease. *Nat Rev Neurosci* 16: 358–372, 2015. doi:10.1038/nrn3880.

37. Pekny M, Pekna M, Messing A, Steinhauser C, Lee JM, Parpura V, Hol EM, Sofroniew MW, Verkhratsky A. Astrocytes: a central element in neurological diseases. *Acta Neuropathol* 131: 323–345, 2016. doi:10.1007/s00401-015-1513-1.

38. Rodríguez-Arellano JJ, Parpura V, Zorec R, Verkhratsky A. Astrocytes in

physiological aging and Alzheimer's disease. *Neuroscience* 323: 170–182, 2016. doi:10.1016/j.neuroscience.2015.01.007.

39. Choi BR, Cho WH, Kim J, Lee JH, Chung C, Jeon WK, Han JS. Increased expression of the receptor for advanced glycation end products in neurons and astrocytes in a triple transgenic mouse model of Alzheimer's disease. *Exp Mol Med* 46: e75, 2014. doi:10.1038/emm.2013.147.

40. Chen Y, Liang Z, Tian Z, Blanchard J, Dai CL, Chalbot S, Iqbal K, Liu F, Gong CX. Intracerebroventricular streptozotocin exacerbates Alzheimer-like changes of 3xTg-AD mice. *Mol Neurobiol* 49: 547– 562, 2014. doi:10.1007/s12035-013-8539-y.

41. Kim D, Cho J, Kang H. Protective effect of exercise training against the progression of Alzheimer's disease in 3xTg-AD mice. *Behav Brain Res* 374: 112105, 2019. doi:10.1016/j.bbr.2019.112105.

42. Mosher KI, Wyss-Coray T. Microglial dysfunction in brain aging and Alzheimer's disease. *Biochem Pharmacol* 88: 594–604, 2014. doi:10.1016/j.bcp.2014.01.008.

43. Zhou L, Huang JY, Zhang D, Zhao YL. Cognitive improvements and reduction in amyloid plaque deposition by saikosaponin D treatment in a murine model of Alzheimer's disease. *Exp Ther Med* 20: 1082– 1090, 2020. doi:10.3892/etm.2020.8760.

44. Bashiri H, Enayati M, Bashiri A, Salari AA. Swimming exercise improves cognitive and behavioral disorders in male NMRI mice with sporadic Alzheimer-like disease. *Physiol Behav* 223: 113003, 2020. doi:10.1016/j.physbeh.2020.113003.

45. Do K, Laing BT, Landry T, Bunner W, Mersaud N, Matsubara T, Li P, Yuan Y, Lu Q, Huang H. The effects of exercise on hypothalamic neurodegeneration of Alzheimer's disease mouse model. *PLoS One* 13: e0190205, 2018. doi:10.1371/journal.pone.0190205.

46. Querfurth HW, LaFerla FM. Alzheimer's disease. *N Engl J Med* 362: 329–344, 2010. [Erratum in *N Engl J Med* 364: 588, 2011]. doi:10.1056/NEJMra0909142.

47. Lim D, Iyer A, Ronco V, Grolla AA, Canonico PL, Aronica E, Genazzani AA. Amyloid b deregulates astroglial mGluR5-mediated calcium signaling via calcineurin and NF-kB. *Glia* 61: 1134–1145, 2013. doi:10.1002/glia.22502.

48. Wood LB, Winslow AR, Proctor EA, McGuone D, Mordes DA, Frosch MP,

Hyman BT, Lauffenburger DA, Haigis KM. Identification of neurotoxic cytokines by profiling Alzheimer's disease tissues and neuron culture viability screening. *Sci Rep* 5: 16622, 2015. doi:10. 1038/srep16622.

49. Wang W, Zhao F, Ma X, Perry G, Zhu X. Mitochondria dysfunction in the pathogenesis of Alzheimer's disease: recent advances. *Mol Neurodegener* 15: 30, 2020. doi:10.1186/s13024-020-00376-6.

50. Abramov AY, Canevari L, Duchen MR. b-amyloid peptides induce mitochondrial dysfunction and oxidative stress in astrocytes and death of neurons through activation of NADPH oxidase. *J Neurosci* 24: 565–575, 2004. doi:10.1523/JNEUROSCI.4042-03.2004.

51. Lustbader JW, Cirilli M, Lin C, Xu HW, Takuma K, Wang N, Caspersen C, Chen X, Pollak S, Chaney M, Trinchese F, Liu S, Gunn-Moore F, Lue LF, Walker DG, Kuppusamy P, Zewier ZL, Arancio O, Stern D, Yan SS, Wu H. ABAD directly links A b to mitochondrial toxicity in Alzheimer's disease. *Science* 304: 448–452, 2004. doi:10.1126/science.1091230.

52. Chin JH, Tse FW, Harris K, Jhamandas JH. b-amyloid enhances intracellular calcium rises mediated by repeated activation of intracellular calcium stores and nicotinic receptors in acutely dissociated rat basal forebrain neurons. *Brain Cell Biol* 35: 173–186, 2007. doi:10. 1007/s11068-007-9010-7.

53. Du H, Yan SS. Mitochondrial permeability transition pore in Alzheimer's disease: cyclophilin D and amyloid b. *Biochim Biophys Acta* 1802: 198–204, 2010. doi:10.1016/j.bbadis.2009.07.005.

54. Du H, Guo L, Fang F, Chen D, Sosunov AA, Mckhann GM, Yan Y, Wang C, Zhang J, Molkentin JD, Gunn-Moore FJ, Vonsattel JP, Arancio O, Chen JX, Yan SD. Cyclophilin D deficiency attenuates mitochondrial and neuronal perturbation and ameliorates learning and memory in Alzheimer's disease. *Nat Med* 14: 1097–1105, 2008. doi:10.1038/nm.1868.

55. Cuadrado-Tejedor M, Vilarino M, Cabodevilla F, Del Río J, Frechilla D, Perez-Mediavilla A. Enhanced expression of the volt- age-dependent anion channel 1 (VDAC1) in Alzheimer's disease transgenic mice: an insight into the pathogenic effects of amyloid-b. *J Alzheimers Dis* 23: 195–206, 2011. doi:10.3233/JAD-2010-100966.

56. Singh P, Suman S, Chandna S, Das TK. Possible role of amyloid-b, adenine nucleotide translocase and cyclophilin-D interaction in mitochondrial dysfunction of Alzheimer's disease. *Bioinformation* 3: 440–445, 2009. doi:10.6026/97320630003440.

57. Manczak M, Anekonda TS, Henson E, Park BS, Quinn J, Reddy PH. Mitochondria are a direct site of A b accumulation in Alzheimer's disease neurons: implications for free radical generation and oxidative damage in disease progression. *Hum Mol Genet* 15: 1437–1449, 2006. doi:10.1093/hmg/ddl066.

58. Opazo C, Huang X, Cherny RA, Moir RD, Roher AE, White AR, Cappai R, Masters CL, Tanzi RE, Indstrosa NC, Bush AI. Metalloenzyme-like activity of Alzheimer's disease b-amyloid. Cu-dependent catalytic conversion of dopamine, cholesterol, and biological reducing agents to neurotoxic H(2)O(2). *J Biol Chem* 277: 40302–40308, 2002. doi:10.1074/jbc.M206428200.

59. Ruthel G, Hollenbeck PJ. Response of mitochondrial traffic to axon determination and differential branch growth. *J Neurosci* 23: 8618– 8624, 2003. doi:10.1523/JNEUROSCI.23-24-08618.2003.

60. Sun T, Qiao H, Pan PY, Chen Y, Sheng ZH. Motile axonal mitochondria contribute to the variability of presynaptic strength. *Cell Rep* 4: 413–419, 2013. doi:10.1016/j.celrep.2013.06.040.

61. Ye M, Chung HS, An YH, Lim SJ, Choi W, Yu AR, Kim JS, Kang M, Cho S, Shim I, Bae H. Standardized herbal formula pm012 decreases cognitive impairment and promotes neurogenesis in the 3xtg ad mouse model of Alzheimer's disease. *Mol Neurobiol* 53: 5401–5412, 2016. doi:10.1007/s12035-015-9458-x.

62. Hu Y, Lai J, Wan B, Liu Z, Zhang Y, Zhang J, Sun D, Ruan G, Liu E, Liu GP, Chen C, Wang DW. Long-term exposure to ELF-MF ameliorates cognitive deficits and attenuates tau hyperphosphorylation in 3xTg AD mice. *Neurotoxicology* 53: 290–300, 2016. doi:10.1016/j. neuro.2016.02.012.

63. Hedberg MM, Clos MV, Ratia M, Gonzalez D, Lithner CU, Camps P, Munoz-Torrero D, Badia A, Gimenez-Llort L, Nordberg A. Effect of huprine X on b-amyloid, synaptophysin and a7 neuronal nicotinic acetylcholine receptors in the brain of 3xTg-AD and APPswe transgenic mice. *Neurodegener Dis* 7: 379–388, 2010. doi:10.1159/000287954.

64. Shruster A, Offen D. Targeting neurogenesis ameliorates danger assessment in a mouse model of Alzheimer's disease. *Behav Brain Res* 261: 193–201, 2014. doi:10.1016/j.bbr.2013.12.028.

65. Prakash A, Kumar A. Role of nuclear receptor on regulation of BDNF and neuroinflammation in hippocampus of b-amyloid animal model of Alzheimer's disease. *Neurotox Res* 25: 335–347, 2014. doi:10.1007/s12640-013-9437-9.

66. Peng S, Wuu J, Mufson EJ, Fahnestock M. Precursor form of brain- derived neurotrophic factor and mature brain-derived neurotrophic factor are decreased in the pre-clinical stages of Alzheimer's dis- ease. *J Neurochem* 93: 1412–1421, 2005. doi:10.1111/j.1471-4159. 2005.03135.x.

67. Moreno-Jimenez EP, Flor-García M, Terreros-Roncal J, Rábano A, Cafini F, Pallas-Bazarra N, Ávila J, Llorens-Martín M. Adult hippocampal neurogenesis is abundant in neurologically healthy subjects and drops sharply in patients with Alzheimer's disease. *Nat Med* 25: 554–560, 2019. doi:10.1038/s41591-019-0375-9.

68. Tobin MK, Musaraca K, Disouky A, Shetti A, Bheri A, Honer WG, Kim N, Dawe RJ, Bennett DA, Arfanakis K, Lazarov O. Human hippocampal neurogenesis persists in aged adults and Alzheimer's dis- ease patients. *Cell Stem Cell* 24: 974–982, 2019. doi:10.1016/j. stem.2019.05.003.

69. Qin XY, Cao C, Cawley NX, Liu TT, Yuan J, Loh YP, Chen Y. Decreased peripheral brain-derived neurotrophic factor levels in Alzheimer's disease: a meta-analysis study (N=7277). *Mol Psychiatry* 22: 312–320, 2017. doi:10.1038/mp.2016.62.

70. Palop JJ, Chin J, Roberson ED, Wang J, Thwin MT, Bien-Ly N, Yoo J, Ho KO, Yu GQ, Kreitzer A, Finkbeiner S, Noebels JL, Mucke L. Aberrant excitatory neuronal activity and compensatory remodeling of inhibitory hippocampal circuits in mouse models of Alzheimer's disease. *Neuron* 55: 697–711, 2007. doi:10.1016/j.neuron.2007.07.025.

71. Stam CJ, van Cappellen van Walsum AM, Pijnenburg YA, Berendse HW, de Munck JC, Scheltens P, van Dijk BW. Generalized synchronization of MEG recordings in Alzheimer's disease: evidence for involvement of the gamma band. *J Clin Neurophysiol* 19: 562–574, 2002. doi:10.1097/00004691-200212000-00010.

72. Verret L, Mann EO, Hang GB, Barth AMI, Cobos I, Ho K, Devidze N, Masliah

E, Kreitzer AC, Mody I, Mucke L, Palop JJ. Inhibitory inter- neuron deficit links altered network activity and cognitive dysfunction in Alzheimer model. *Cell* 149: 708–721, 2012. doi:10.1016/j. cell.2012.02.046.

73. Gillespie AK, Jones EA, Lin YH, Karlsson MP, Kay K, Yoon SY, Tong LM, Nova P, Carr JS, Fank LM, Huang Y. Apolipoprotein E4 causes age-dependent disruption of slow gamma oscillations during hippocampal sharp-wave ripples. *Neuron*. 90: 740–751, 2016. doi:10.1016/j.neuron.2016.04.009.

74. Klein AS, Donoso JR, Kempter R, Schmitz D, Beed P. Early cortical changes in gamma oscillations in Alzheimer's disease. *Front Syst Neurosci* 10: 83, 2016. doi:10.3389/fnsys.2016.00083.

75. Kurudenkandy FR, Zilberter M, Biverstål H, Presto J, Honcharenko D, Stromberg R, Johansson J, Winblad B, Fisahn A. Amyloid- b-induced action potential desynchronization and degradation of hippocampal gamma oscillations is prevented by interference with peptide conformation change and aggregation. *J Neurosci* 34: 11416–11425, 2014. doi:10.1523/JNEUROSCI.1195-14.2014.

76. Whittaker RG, Turnbull DM, Whittington MA, Cunningham MO. Impaired mitochondrial function abolishes gamma oscillations in the hippocampus through an effect on fast-spiking interneurons. *Brain* 134: e180, 2011. doi:10.1093/brain/awr018.

77. Goutagny R, Gu N, Cavanagh C, Jackson J, Chabot JG, Quirion R, Krantic S, Williams S. Alterations in hippocampal network oscillations and theta-gamma coupling arise before Ab overproduction in a mouse model of Alzheimer's disease. *Eur J Neurosci* 37: 1896–1902, 2013. doi:10.1111/ejn.12233.

78. Adaikkan C, Middleton SJ, Marco A, Pao PC, Mathys H, Kim DNW, Gao F, Young JZ, Suk HJ, Boyden ES, McHugh TJ, Tsai LH. Gamma entrainment binds higher-order brain regions and offers neuroprotection. *Neuron* 102: 929–943.e8, 2019. doi:10.1016/j. neuron.2019.04.011.

79. Cass SP. Alzheimer's disease and exercise: a literature review. *Curr Sports Med Rep* 16: 19–22, 2017. doi:10.1249/JSR.0000000000000332.

80. García-Mesa Y, Lopez-Ramos JC, Gimenez-Llort L, Revilla S, Guerra R, Gruart A, Laferla FM, Cristofol R, Delgado-García JM, Sanfeliu C. Physical exercise protects against Alzheimer's disease in 3xTg-AD mice. *J Alzheimers Dis* 24: 421–454,

2011. doi:10.3233/ JAD-2011-101635.

81. Brown BM, Peiffer JJ, Taddei K, Lui JK, Laws SM, Gupta VB, Taddei T, Ward VK, Rodrigues MA, Burnham S, Rainey-Smith SR, Villemagne VL, Bush A, Ellis KA, Masters CL, Ames D, Macaulay SL, Szoeke C, Rowe CC, Martins RN; for the AIBL Research Group. Physical activity and amyloid-b plasma and brain levels: results from the Australian Imaging, Biomarkers and Lifestyle Study of Ageing. *Mol Psychiatry* 18: 875–881, 2013. doi:10.1038/mp.2012.107.

82. Brown BM, Sohrabi HR, Taddei K, Gardener SL, Rainey-Smith SR, Peiffer JJ, Xiong C, Fagan AM, Benzinger T, Buckles V, Erickson KI, Clarnette R, Shah T, Masters CL, Weiner M, Cairns N, Rossor M, Graff-Radford NR, Salloway S, Voglein J, Laske C, Noble J, Schofield PR, Bateman RJ, Morris JC, Martins RN; Dominantly Inherited Alzheimer Network. Habitual exercise levels are associated with cerebral amyloid load in presymptomatic autosomal dominant Alzheimer's disease. *Alzheimers Dement* 13: 1197–1206, 2017. doi:10.1016/j.jalz.2017.03.008.

83. Liu Y, Chu JMT, Yan T, Zhang Y, Chen Y, Chang RCC, Wong GTC. Short-term resistance exercise inhibits neuroinflammation and attenuates neuropathological changes in 3xTg Alzheimer's disease mice. *J Neuroinflammation* 17: 4, 2020. doi:10.1186/s12974-019-1653- 1657.doi:10.1186/s12974-019-1653-7.

84. Leem YH, Lee YI, Son HJ, Lee SH. Chronic exercise ameliorates the neuroinflammation in mice carrying NSE/htau23. *Biochem Biophys Res Commun* 406: 359–365, 2011. doi:10.1016/j.bbrc.2011.02.046.

85. Marques-Aleixo I, Santos-Alves E, Balça MM, Rizo-Roca D, Moreira PI, Oliveira PJ, Magalhães J, Ascensão A. Physical exercise improves brain cortex and cerebellum mitochondrial bioenergetics and alters apoptotic, dynamic and auto(mito)phagy markers. *Neuroscience* 301: 480–495, 2015. doi:10.1016/j.neuroscience.2015.06.027.

86. Seo JH, Park HS, Park SS, Kim CJ, Kim DH, Kim TW. Physical exercise ameliorates psychiatric disorders and cognitive dysfunctions by hippocampal mitochondrial function and neuroplasticity in post-traumatic stress disorder. *Exp Neurol* 322: 113043, 2019. doi:10.1016/j. expneurol.2019.113043.

87. Um HS, Kang EB, Koo JH, Kim HT, Lee J, Kim EJ, Yang CH, An GY, Cho

IH, Cho JY. Treadmill exercise represses neuronal cell death in an aged transgenic mouse model of Alzheimer's disease. *Neurosci Res* 69: 161–173, 2011. doi:10.1016/j.neures.2010.10.004.

88. Baek SS, Kim SH. Treadmill exercise ameliorates symptoms of Alzheimer disease through suppressing microglial activation- induced apoptosis in rats. *J Exerc Rehabil* 12: 526–534, 2016. doi:10.12965/jer.1632858.429.

89. Markham A, Cameron I, Franklin P, Spedding M. BDNF increases rat brain mitochondrial respiratory coupling at complex I, but not complex II. *Eur J Neurosci* 20: 1189–1196, 2004. doi:10.1111/j.1460- 9568.2004.03578.x.

90. Gomez-Pinilla F, Ying Z, Roy RR, Molteni R, Edgerton VR. Voluntary exercise induces a BDNF-mediated mechanism that pro- motes neuroplasticity. *J Neurophysiol* 88: 2187–2195, 2002. doi:10.1152/jn.00152.2002.

91. Adlard PA, Perreau VM, Cotman CW. The exercise-induced expression of BDNF within the hippocampus varies across life-span. *Neurobiol Aging* 26: 511–520, 2005. doi:10.1016/j.neurobiolaging.2004.05.006.

92. Kovalchuk Y, Hanse E, Kafitz KW, Konnerth A. Postsynaptic induction of BDNF-mediated long-term potentiation. *Science* 295: 1729– 1734, 2002. doi:10.1126/science.1067766.

93. Martin JL, Finsterwald C. Cooperation between BDNF and gluta- mate in the regulation of synaptic transmission and neuronal development. *Commun Integr Biol* 4: 14–16, 2011. doi:10.4161/cib.13761.

94. Cho J, Shin MK, Kim D, Lee I, Kim S, Kang H. Treadmill running reverses cognitive declines due to Alzheimer disease. *Med Sci Sports Exerc* 47: 1814–1824, 2015. doi:10.1249/MSS.0000000000000612.

95. Revilla S, Sunol C, García-Mesa Y, Gimenez-Llort L, Sanfeliu C, Cristo□fol R. Physical exercise improves synaptic dysfunction and recovers the loss of survival factors in 3xTg-AD mouse brain. *Neuropharmacology* 81: 55–63, 2014. doi:10.1016/j.neuropharm.2014.01.037.

96. Choi SH, Bylykbashi E, Chatila ZK, Lee SW, Pulli B, Clemenson GD, Kim E, Rompala A, Oram MK, Asselin C, Aronson J, Zhang C, Miller SJ, Lesinski A, Chen JW, Kim DY, van Praag H, Spiegelman BM, Gage FH, Tanzi RE. Combined adult neurogenesis

and BDNF mimic exercise effects on cognition in an Alzheimer's mouse model. *Science* 361: eaan8821, 2018. doi:10.1126/science.aan8821.